Ecological Divergence and the History of Gene Flow in the Nearctic Milksnakes (*Lampropeltis triangulum* Complex)

Frank T. Burbrink[1]*, Justin M. Bernstein[2], Arianna Kuhn[1], Marcelo Gehara[3], and Sara Ruane[3,4]

[1]*Department of Herpetology, American Museum of Natural History, Central Park West at 79th Street, New York, NY 10024, USA;*
[2]*Department of Biological Sciences, Rutgers University Newark, 195 University Ave, Newark, NJ 07102, USA;*
[3]*Department of Earth and Environmental Sciences, Rutgers University Newark, 195 University Ave, Newark, NJ 07102, USA;*
[4]*Amphibian and Reptile Collection, Negaunee Integrative Research Center, Field Museum of Natural History, 1400 S Lake Shore Dr, Chicago, IL 60605, USA*
*Correspondence to be sent to: Department of Herpetology, American Museum of Natural History, Central Park West at 79th Street, New York, NY 10024, USA;
E-mail: fburbrink@amnh.org.

Abstract.—Many phylogeographic studies on species with large ranges have found genetic–geographic structure associated with changes in habitat and physical barriers preventing or reducing gene flow. These interactions with geographic space, contemporary and historical climate, and biogeographic barriers have complex effects on contemporary population genetic structure and processes of speciation. While allopatric speciation at biogeographic barriers is considered the primary mechanism for generating species, more recently it has been shown that parapatric modes of divergence may be equally or even more common. With genomic data and better modeling capabilities, we can more clearly define causes of speciation in relation to biogeography and migration between lineages, the location of hybrid zones with respect to the ecology of parental lineages, and differential introgression of genes between taxa. Here, we examine the origins of three Nearctic milksnakes (*Lampropeltis elapsoides*, *Lampropeltis triangulum* and *Lampropeltis gentilis*) using genome-scale data to better understand species diversification. Results from artificial neural networks show that a mix of a strong biogeographic barrier, environmental changes, and physical space has affected genetic structure in these taxa. These results underscore conspicuous environmental changes that occur as the sister taxa *L. triangulum* and *L. gentilis* diverged near the Great Plains into the forested regions of the Eastern Nearctic. This area has been recognized as a region for turnover for many vertebrate species, but as we show here the contemporary boundary does not isolate these sister species. These two species likely formed in the mid-Pleistocene and have remained partially reproductively isolated over much of this time, showing differential introgression of loci. We also demonstrate that when *L. triangulum* and *L. gentilis* are each in contact with the much older *L. elapsoides*, some limited gene flow has occurred. Given the strong agreement between nuclear and mtDNA genomes, along with estimates of ecological niche, we suggest that all three lineages should continue to be recognized as unique species. Furthermore, this work emphasizes the importance of considering complex modes of divergence and differential allelic introgression over a complex landscape when testing mechanisms of speciation. [Cline; delimitation; Eastern Nearctic; Great Plains; hybrids; introgression; speciation.]

Speciation usually begins with spatial isolation or adaptation to unique environments without strict isolation (Schilthuizen 2000). For many organisms, a mix of environmental changes and strong geographic barriers to dispersal have structured populations and generated species (Endler 1977; Avise 2000; Pyron and Burbrink 2010; Wollenberg et al. 2019). Isolation can be complete in the case of allopatry or partial in the case of parapatry. These mechanisms of complete or partial isolation are likely the most common processes of divergence, at least in vertebrates (Kozak and Wiens 2006; Fitzpatrick et al. 2009; Nosil 2012; Edwards et al. 2020). Complete spatial isolation and subsequent formation of unique lineages may be due to isolation or long-range dispersal across barriers such as mountains, rivers, or other intervening unsuitable habitats (Mayr 1963; Avise 2000; Rundle and Nosil 2005; Schluter 2009; Pyron and Burbrink 2009). Adaptation to unique habitats may also occur along with isolation, and Dobzhansky–Muller processes associated with drift may enhance genetic disconnection upon secondary contact (Dobzhansky 1937; Muller 1942; Orr and Turelli 2001).

In contrast, parapatric speciation occurs contiguously over the landscape where lineages adapt to spatially exclusive habitats (Fisher 1930; Endler 1977; Coyne and Orr 2004; Schluter 2009). This mode of speciation initially involves only key parts of the genome associated with adaptation to different environments and may promote the formation of genomic islands. Early in parapatric speciation, a large portion of alleles move freely across contact zones whereas a smaller number of locally adapted alleles fail to introgress between lineages (Hendry et al. 2007; Harrison and Larson 2014; Stankowski et al. 2019). Alternatively, under a changing and dynamic environment, adaptive introgression may provide new traits to better fit local conditions (Abbott et al. 2013; Bierne et al. 2013; Ma et al. 2019), reducing the possibility of extinction of the receiver. It is therefore now widely recognized that speciation with gene flow and reticulate evolution is common throughout the tree of life when compared to pure allopatry (Ackermann and Bishop 2010; Nosil and Feder 2012; Janèúchová-Lásková et al. 2015; Payseur and Rieseberg 2016; Kumar et al. 2017; Mason et al. 2019; Dong et al. 2020). Over long periods of time, divergences initiated via parapatry may rapidly become allopatric, and allopatrically diverging populations may have subsequently been forced into secondary contact.

Periods of isolation or partial isolation and reconnection must have been common throughout the changing environments of the Pleistocene, particularly in the Northern Hemisphere. Indeed, this model of mixing, isolation, and mixing (MIM) has been proposed to account for rapid diversification of species in areas where long-term allopatry is unexpected (He et al. 2019).

With numerous biogeographic barriers, changes in environment, and Pleistocene glacial cycles, the forested regions of eastern North America north of Mexico (Eastern Nearctic; ENA) have played a strong role in formation and maintenance of lineages among many unrelated taxa. (Mayden 1988; Avise 1992; Soltis et al. 2006). In many cases, the combined effects of these environmental and biogeographic barriers have isolated populations and formed lineages (species) across unrelated groups (Soltis et al. 2006; Wieringa et al. 2020). Barriers in the ENA are typically associated with changes in habitat and the formation of suture zones between taxa (Savage 1960; Remington 1968). Major barriers here include the inundation of Florida into islands and subsequent reconnection to the continental United States, elevation at the Appalachians, and isolation at southeastern river systems and the Mississippi River (Walker and Avise 1998; Burbrink et al. 2000; Leaché et al. 2002; Jaeger et al. 2005; Rissler and Smith 2010; Zellmer et al. 2012; Burbrink and Guiher 2015; Wieringa et al. 2020). Environmental changes in precipitation occur on an east–west axis with associated habitats changing from forests to the flat, high plateau of grasslands ranging west of the Mississippi River to the Rocky Mountains, known as the Great Plains (GP; Axelrod 1985; Bailey 1995; Costa et al. 2008). Additionally, for those taxa not adapted to cold climates, repeated glacial cycling during the Pleistocene has a noted influence on biodiversity by reducing optimal habitats and isolating or compressing taxa into southern refugia. This is typically followed by population expansion upon return of favorable northern climates (Klicka and Zink 1999; Hewitt 2000, 2004, 2011; Waltari et al. 2007; Bintanja and Van De Wal 2008; Abe-Ouchi et al. 2013; Ruane et al. 2015; Burbrink et al. 2016). North America experienced multiple 100 ky glacial cycles starting at the mid-Pleistocene Transition (~1 mya; Bintanja and Van De Wal 2008), which necessarily shifted ranges of many species several times. Ironically, the identity of many closely related species or lineages have been maintained over this long time frame despite recurrent episodes of gene flow (Burbrink et al. 2021). While all of these environmental, physical, and spatial variables have had obvious effects on the genetic-spatial structure and species turnover in this area (Rising 1983; Swenson 2006; Fontanella et al. 2008; Placyk et al. 2012; Reding et al. 2012; Burbrink and Guiher 2015; Burbrink and Myers 2015), genome-scale studies assessing the independent effects of these variables are lacking.

To better understand the diversification in the ENA, we establish a methodological pipeline to address questions about the formation and maintenance of species in the Nearctic milksnake complex. The milksnakes in general (and including the Mexican kingsnakes) are widely distributed from Canada to Ecuador but show deep phylogeographic structure in the eastern United States, particularly near the intersection of the GP and ENA and in the Southeast (Burbrink and Gehara 2018). Previously, Ruane et al. (2014) demonstrated three unique species occurring in the United States: *Lampropeltis elapsoides* in the southeast, *Lampropeltis triangulum* in the forested areas of the east and north, and *Lampropeltis gentilis* mostly in the grasslands and more arid regions of the western United States. Because these snakes occupy a complex region composed of conspicuous changes in precipitation and temperature, physical barriers to dispersal, and glacial cycles altering ranges, we hypothesize that combinations of these variables have contributed to structuring species over the landscape and have had significant effects on historical demography.

Our methodology focuses on the following categories to understand the formation of species by: i) identifying and validating the existence of lineages and their ranges, ii) testing models of divergence, iii) isolating the effects of spatial, environmental, and biogeographic barriers on lineage structure, and iv) examining genomic interactions in zones of contact. We first examine the presence of unique lineages and separate these from the spurious groupings due to isolation by distance (IBD) and allele surfing. The former predicts that migration among populations decreases as spatial distance between populations increases (Wright 1943; Slatkin 1993; Guillot and Rousset 2013; Seeholzer and Brumfield 2018); this can lead to incorrectly inferring lineages that are distinct when intermediate populations are poorly sampled. Allele surfing happens when particular alleles reach high frequencies in rapidly expanding populations (Klopfstein et al. 2006; Excoffier and Ray 2008) which can give the appearance of unique and strongly sorting groups (Streicher et al. 2016). Second, we use isolation and migration techniques (Hey 2010; He et al. 2019) in the form of approximate Bayesian computation (ABC) and artificial neural network (ANN) models to test i) if populations formed in the Pleistocene, ii) if populations identified herein show complete isolation, periodic isolation, or no isolation, and iii) if population sizes changed over the Pleistocene as would be predicted given the number of glacial cycles. Third, we use another ANN method to then tease out the effects of spatial distance, changing precipitation and temperature over space, and biogeographic barriers on phylogeographic structure. Given results from the isolation–migration models, it is expected that if these species formed in strict allopatry, then only hard and continuous biogeographic barriers are responsible for the formation of lineages. Alternatively, in cases where gene flow occurs constantly over time or only in secondary contact, then a mix of spatial and environmental change and biogeographic barriers are likely responsible for genetic structure. Where we find a spatial connection between species, we then hypothesize that differential introgression of alleles has occurred. Where alleles show narrow cline widths over geographic distance, we expect that the turnover

in these alleles will be associated with similar changes in environment and high F_{ST} values. We then compare this to various processes of diversification. Finally, we examine population demography in combination with environmental niche models to understand the effects of Pleistocene climate change on population sizes and location of species. We hypothesize that where models show compression of suitable habitat during glacial maxima and expansion of habitat during glacial retreat, we will find increases in effective population sizes towards contemporary times. Ultimately, this research allows us to better comprehend both the effects of past and current environment on the genetic structure within and among species and differential introgression across the transition between the ENA and GP, a broad barrier separating Eastern and Central North America.

MATERIALS AND METHODS

Data

We sampled a total of 190 individuals from four milksnake taxa, *Lampropeltis elapsoides, L. triangulum, L. gentilis*, and *L. annulata*, from our own field collections, museum collections, and personal loans of tissues from individuals (Electronic Supplementary Material Data D1). Our sampling liberally covers the ranges of *L. elapsoides, L. triangulum,* and *L. gentilis* (Fig. 1). We also sampled four individuals from the species, *L. annulata*, which may be the sister species to *L. gentilis*. *Lampropeltis annulata* was excluded from several analyses where low sample sizes would not allow for accurate parameter estimations or when not the focus of a specific test as noted. We underscore that *L. elapsoides* is not generally considered a contentious species and that it may be the sister taxon to the *L. triangulum* + *L. gentilis* group or alternately, the Mexican kingsnake group (Ruane et al. 2014; Chen et al. 2017; Burbrink and Gehara 2018). However, reports of some limited gene flow between *L. elapsoides* and *L. triangulum* (Armstrong et al. 2001) indicate that exploring historical demography and migration among these three snakes is important to understand species boundaries among them.

High molecular weight DNA was obtained using the Qiagen DNEasy Blood & Tissue and MagAttract HMW DNA Kits (Qiagen). DNA concentrations were quantified with a Qubit 3.0 Fluorometer (Thermo Fisher Scientific, Waltham, MA, USA) using the Qubit dsDNA BR Assay Kit (Thermo Fisher Scientific). Libraries were prepared following the genotype by sequencing (GBS) protocol of Elshire et al. (2011) at the University of Wisconsin (UW) Biotechnology DNA Sequencing Facility. Genomic DNA was digested using the restriction enzyme ApeKI (cut site: G/CWGC), and libraries were sequenced on an Illumina NovaSeq 6000 yielding 150 bp paired-end reads. Raw reads were processed and output files were generated using the bioinformatic pipeline ipyrad v0.9.42 (Eaton and Overcast 2020; see Text S1
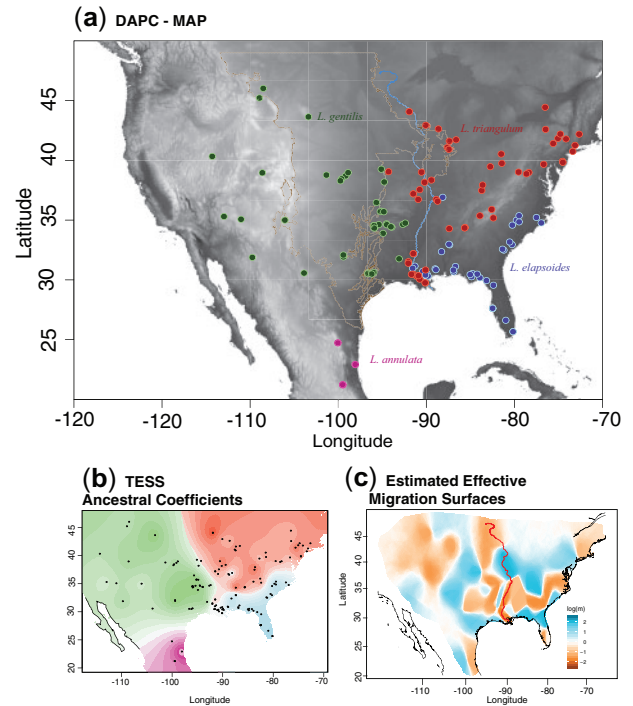

FIGURE 1. Population clustering and phylogenetic methods for four Nearctic milksnake taxa (*Lampropeltis*) showing a) population structure over space using DAPC displaying the location of the Mississippi River (blue) and the boundary of the Great Plains (brown), b) TESS3r estimates of coefficients of ancestry over space, and c) estimated effective migration surfaces (EEMS) with areas of high (blue) and low (brown) migration. Here, red = *L. triangulum*, blue = *L. elapsoides*, green = *L. gentilis*, purple = *L. annulata*.

of the Supplementary material available on Dryad at http://dx.doi.org/10.5061/dryad.g79cnp5qm). Individuals and loci with excessively high missing data were removed but those with enough signal were retained for subsequent analyses. We filtered the final assembly in R using a custom script that draws a single biallelic polymorphic site per locus with the least amount of missing data across individuals. This eliminated loci missing across >90% of individuals and individuals with >70% missing loci. These data are used in specific downstream analyses that could be biased by redundant signal from linked SNPs or excessive missing data.

Geographic Groupings and Phylogenomic Structure

For all samples, we explored three different methods to group individuals into lineages using the SNP data set: discriminant analysis of principal components (DAPC; Jombart et al. 2010), TESS3r (Caye et al. 2016), and sparse nonnegative matrix factorization (SNMF; Frichot et al. 2014). We compare groupings among these methods given that their assumptions about population structure differ. These groupings were then used for downstream testing of process of divergence and allelic introgression. To visualize the spatial distribution of

genetic differentiation while explicitly accounting for IBD, we used effective migration surfaces (EEMS) to estimate migration rates over the landscape (see Text S1 of the Supplementary material available on Dryad for details on these methods). We also calculated overall F_{ST} among groups and for each locus.

To determine if these groupings represent unique evolutionary lineages, we estimated coalescent-based phylogenetic relationships in the SNAPP v1.5.1 module (Bryant et al. 2012) in BEAST v2.5.2 (Bouckaert et al. 2014). Because SNAPP cannot use the full data set, we selected four individuals from each group as assigned by DAPC, three different times. These were sampled incrementally from the zone of connection between taxon pairs to within each parental range (for details running SNAPP please see Text S1 of the Supplementary material available on Dryad). We tested three alternative speciation scenarios: i) all four taxa (*L. triangulum, L. gentilis, L. annulata,* and *L. elapsoides*) were delimited and compared to ii) only three taxa, where *L. annulata* and *L. gentilis* were collapsed, iii) only two taxa where *L. triangulum, L. gentilis,* and *L. annulata* were collapsed (*L. elapsoides* was never collapsed for any scenario). We also compared the full model with four taxa to one where we shuffled individuals between *L. triangulum* and *L. gentilis* to demonstrate that these were not spurious groupings. We used a stepping-stone analysis with *PathSampleAnalyser* with 72 steps and a chain length of 1×10^6 and burnin percentage set at 50%. Stationarity was confirmed with estimated sample size (ESS) > 200 for the log likelihood of each step using Tracer v1.7.1 (Drummond and Rambaut 2007).

Tree Structure

To further examine the clustering by geography, understand the relationships among groups, and assess reciprocal monophyly, we concatenated phased GBS loci resulting in an alignment with a length of 233,540 bp for 288 samples (phased from 144 individuals). We estimated a maximum likelihood (ML) phylogeny using IQ-Tree (Nguyen et al. 2015) with 1000 ultrafast nonparametric bootstraps using the GTR+Γ+I model. We also grouped all individuals within their predicted species following DAPC results and ran the polymorphism aware model (PoMo) in IQ-Tree to account for lineage sorting and provide a stable topology for downstream demographic analyses.

Congruence between mtDNA and GBS Data

The mtDNA genome is unlinked to the GBS data and we therefore examined congruence between GBS clusters and mtDNA tree structure. We determined if resulting geographic structure using mtDNA data taken from many of these same individuals of *L. gentilis, L. triangulum, L. elapsoides,* and *L. annulata* in Ruane et al. (2014) was comparable to our GBS cluster estimates (Figs. 1 and 2). Using 206 samples of milksnakes for

cytochrome b (cytb; 1117 bp) from Ruane et al. (2014), we estimated phylogeographic structure in IQ-Tree (Nguyen et al. 2015) assessing 279 substitution models using AIC and BIC measures of support. We determined node support by bootstrapping these data 1000 times and re-estimating the tree under the preferred model for each replicate. We compared the mtDNA groupings to those directly from the DAPC group assignments using a Fisher's exact test on a 4×4 table showing matches for each mtDNA clade and GBS grouping.

Allele Surfing

Because lack of heterozygosity for one of the lineages at the expanding front of a population could produce spurious groupings, we tested for the presence of allele surfing between *L. triangulum* and *L. gentilis*. We specifically tested allele surfing following Pereira et al. (2018) and grouped individuals into 18 nearest populations (3–20 individuals per population) from east to west across North America covering the ranges of both *L. triangulum* and *L. gentilis* (Fig. S1 of the Supplementary material available on Dryad) and estimated heterozygosity for each locus. We then tested correlation between heterozygosity and longitude. Where we found significant correlation, we inspected estimates to determine fixed differences in heterozygosity between taxa.

Timing of Origin, Migration, and Historical Demography

With the population assignment of the milksnakes established, we estimated timing of divergence, historical and contemporary rates of migration, and changes in population size through time for *L. gentilis, L. triangulum,* and *L. elapsoides*. We tested three competing demographic hypotheses, all with the same fixed topology estimated from the PoMo model. For the simplest hypothesis, we assumed an isolation with migration model with constant population size (IM); the second hypothesis assumed an isolation with migration model with one demographic change in each species (IMD); and the third hypothesis consisted of an isolation with migration model including two demographic changes separated in time for each species which generated a demographic bottleneck history (IMBott), as might be expected given Pleistocene climatic changes. We also tested alternative versions of these three hypotheses where migration parameters were constrained to secondary contact starting after the Last Glacial Maximum (LGM, min:1, max 21 Kya; IM-sc, IMD-sc, IMBott-sc; Fig. 3). We used a generation time prior of 2.5 years (Ernst and Ernst 2003; Ruane et al. 2014; Chen et al. 2017; Burbrink and Gehara 2018), and we accounted for mutation rate variation by sampling from a normal distribution with a mean of rates of substitution at a mean of 6×10^{-9} per site per generation (standard deviation $= 1 \times 10^{-9}$;

(a) Concatenated GBS Phylogeny   **(b) mtDNA (cytb) Phylogeny**   **(c) Contigency Table**
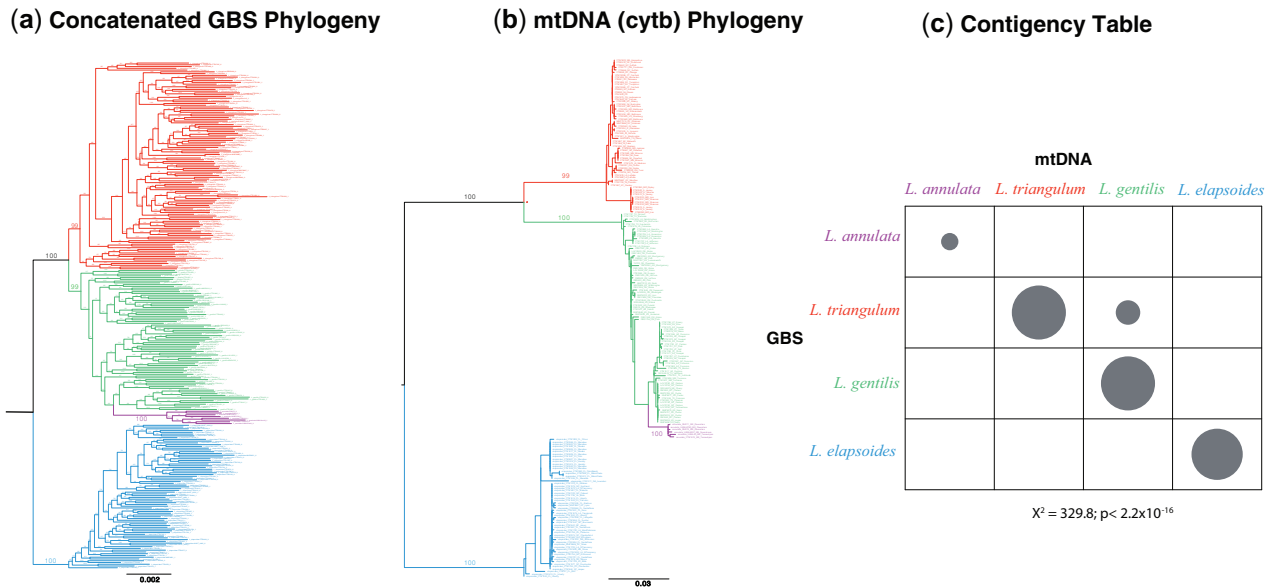

FIGURE 2.   Phylogenies for Nearctic milksnake taxa (*Lampropeltis*): a) concatenated GBS data and b) mtDNA data showing colors for the four clades and species with branch numbers representing nonparametric bootstrap support. c) Contingency table showing agreement between GBS and mtDNA groupings of individuals by clade and X^2 significance. Colors on clades in the trees correspond to those same taxa identified on the margins of the contingency table.

Harrington et al. 2018; Myers et al. 2020). For each model, we used PipeMaster 0.0.9 Gehara et al. 2020; https://github.com/gehara/PipeMaster) to sample demographic parameters from prior distributions (see Supplementary material available on Dryad for a full list of priors) and simulated 10,000 data sets of 74 summary statistics (mean and variance for each species and overall: number of segregating sites, nucleotide diversity, Watterson's Θ, Tajima's D, F_{ST}, number of haplotypes, haplotype diversity, pairwise shared polymorphism, fixed polymorphism, and private polymorphism). PipeMaster uses the program ms (Hudson 2002), which simulates coalescent trees of haploid chromosomes scaled to the population parameter *theta*, and randomly places mutations on these trees according to the infinite site model (Hudson 1983). Also, since the simulated summary statistics represented the average and variance across all loci, we included all sequenced loci and their entire length (instead of a single SNP), totaling 3734 loci. Similarly, for the observed data, we retained the entire sequence for each locus. Therefore, after phasing all loci using ipyrad, we eliminated individuals for each locus with any missing sites. This preserved complete genome-wide variation (i.e., no missing data per locus). Before proceeding with the model inference, we reduced the empirical data to the same 74 summary statistics and calculated a principal component analysis to ensure that the empirical data was contained within the range of the simulated data. We then used the simulated data to train an artificial neural network (ANN) classification model using the R interface from Keras (Chollet 2015; for

details on running the ANN with PipeMaster see Text S1 of the Supplementary material available on Dryad).

Spatial–Environmental Population Genetics

We used a combination of redundancy analyses (RDA; Legendre et al. 2011; Diniz-Filho et al. 2013) and artificial neural networks (ANN; Lek and Guégan 1999; Legendre and Fortin 2010; Legendre et al. 2011) to examine the effects of climate, space, and biogeographic barriers on genetic population structure, explicitly accounting for IBD. We used two data sets, one with all samples across the four taxa and one comparing only the sister species *L. gentilis* and *L. triangulum*. We calculated Euclidian genetic distance as our response variable for RDA analyses and subsequent transformations of this (see below) for ANN in R. Our first set of predictor variables used georeferenced samples to calculate geographic distances using pairwise great-circle distances among all points using the R package fossil (Vavrek 2020). To better understand the complexity of how these geographic distances interact with genetic structure, we transformed spatial distance between all samples using principal coordinates neighbor matrices (PCNM) in the R package vegan (Dixon 2003). This accounts for multiple spatial structures (neighborhoods) that helped identify nonspatial effects on genetic structure when used with other predictors (Borcard and Legendre 2002). To understand the effect of these other typically nonspatial variables on genetic structure, we used the R package raster (Hijmans et al. 2014) to extract from each georeferenced sample i) elevation, ii) current climate
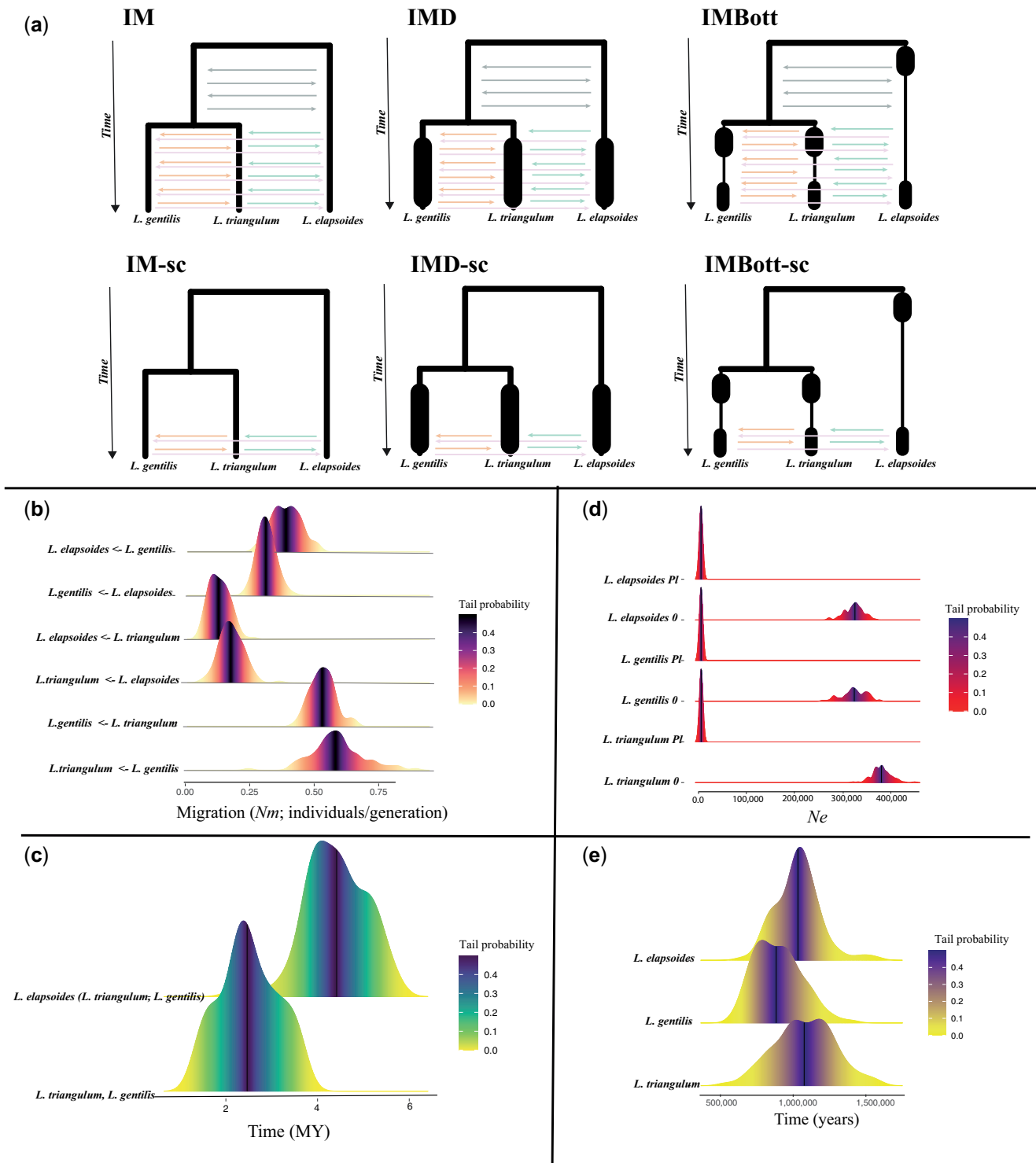
FIGURE 3. a) Models of species divergence for Nearctic milksnake taxa (*Lampropeltis*) tested here using PipeMaster (see text), where population-size changes are represented by differences in branch thickness and horizontal arrows represents migration between taxa. Historical demographic estimates from the best supported model reflecting isolation and migration with population size changes: b) migration rates (*Nm*), c) timing of divergence, d) population size changes (*Ne*) from the Pleistocene (Pl) to contemporary times (0), and e) timing of population size changes.

(obtained from PaleoClim database; Brown et al. 2018), iii) east or west orientation to the Mississippi River (MR) and east and west orientation to the Great Plains (GP; defined in Hanberry 2019). We note that for snakes and other organisms in this region, population structure has often been defined by the MR (Burbrink et al. 2000,

2008; Brandley et al. 2010; Pyron and Burbrink 2010). We removed correlated bioclimatic variables ($\rho > 0.90$). We used RDA to examine the effect of climate, elevation, MR, and GP on genetic structure while isolating (partialing out) the effects of geographic space using the *capscale* function in vegan and then calculated significance using ANOVA (Legendre et al. 2011; Diniz-Filho et al. 2013).

We compared the results from RDA to ANN. Using ANN, we examined the overall accuracy of these models and the influence of the same predictor variables on genetic structure of the milksnakes. This ANN method assesses overall model accuracy over a range of variable types and predicts importance of each variable independently (Lek et al. 1996; Zhang 2010; Libbrecht and Noble 2015; Sheehan et al. 2016). We used principal coordinates analyses (PCoA; Gower 1966) in the R package adegenet to convert genetic distances into 10 orthogonal axes. We applied regression-based ANN to identify which geographic spatial variables, environment, and MR and GP barrier variables predicted genetic distances and then ranked those based on order of model importance. We used the R package caret (Kuhn 2008) to run the ANN regression by partitioning the data into the standard 70% training and 30% test sets (Lek et al. 1996; Zhang 2010; Burbrink et al. 2020). A total of 1000 maximum iterations were run to guarantee convergence and we resampled the data using the default 25 bootstrap replicates to reach convergence across the following parameters: weight decay, RMSE, r^2, and mean absolute error. We assessed variance in accuracy by repeating these analyses 100 times randomly recomposing the test and training data set. Accuracy was compared to an ANN run where response variables were randomly shuffled to determine where accuracy on the unshuffled data converged on these random predictions. This helped determine how many axes of genetic variation were meaningfully predicted by the independent variables. We also compared results from our ANN analysis to those using RDA.

GBS Clinal Analyses

To estimate the geographic gradient of genomic differences between adjacent taxa, we calculated the steepness of cline of these differences to generate the width of the cline, where steeper clines have relatively narrower widths. We determined the width of clines between *L. gentilis* and *L. triangulum* and between *L. triangulum* and *L. elapsoides*. According to the literature in some areas, *L. triangulum* and *L. elapsoides* occur sympatrically, potentially with minimal gene flow (Armstrong et al. 2001). Therefore, clinal estimates could vary by location. All two-dimensional georeferenced samples were reduced to a single dimension appropriate for clinal analyses in HZAR (Derryberry et al. 2014) by i) estimating the division between species using admixture proportions from TESS3r and interpolating these over space to determine the probable cline center using the Akima package (Akima et al. 2016), ii) taking the geographic distance between each sample and the

center of the hybrid zone, and iii) assigning a positive or negative sign to these distances depending on individual orientation to the line of admixture. We used admixture proportions and distances to fit five sigmoidal clinal models in HZAR under the Gaussian cline model to estimate width and center: i) no tails, ii) right tail only, iii) left tail only, iv) mirrored tails, and v) both tails estimated independently (see Derryberry et al. 2014). We also fit clines to environmental distances by converting the admixed hybrid-zone line and all sampled points using current climate data while eliminating correlated variables and reducing dimensionality using PCA (as described above using RDA). We then estimated absolute Euclidian environmental distance from each sample to the admixture line and placed the proper sign depending on orientation to the hybrid zone. We fit both geographic and environmental distance clines to all five tailed models using AICc, running the MCMC chains for 5×10^6 generations, thinning by 5×10^3 generations, and estimating stationarity using ESS >200 in the R package CODA (Plummer et al. 2006).

We estimated cline width and center for each locus using HZAR given individual allele frequency and as described above, distance and orientation to the admixture line. For each locus, we estimated fixation (>0.80) in 5% of each cline tail representing parental lineages. We also estimated cline width for each locus and compared these to estimates of width from neutral cline predictions following the equation from Barton and Gale (1993): $w = 2.51\sigma\sqrt{T}$. Here, root mean squared (RMS) maximum lifetime dispersal $=\sigma$ and generation times since the origin of each sister pair $=T$. Lifetime dispersal for most snakes is unknown, however long distance movements of 0.4 km within a few months in regions constrained to hibernacula have been documented for milksnakes (Fitch and Fleet 1970; Fitch 1999). In the southern portions of their range, where snakes are not constrained to hibernacula, movements throughout a season may be greater. We therefore used conservative estimates of RMS maximum lifetime dispersal estimates of 1–4 km. For predicting time since the formation of hybrid zones, we estimated that these contact zones have likely existed since the Pleistocene given measures that predict constant gene flow through time and timing of population expansion (see below).

mtDNA and GBS Spatial Concordance

To assess spatial congruence with the GBS data, we first used the predicted estimate of hybrid zone centers between pairs of taxa using spatial contours from the TESS3r estimates for ancestral coefficients. With these boundaries between GBS clusters established, we determined the significance of individuals fitting to mtDNA clades on either side of this boundary using Fisher's exact test. For example, using the mtDNA clade designations, we calculated how often individuals from *L. triangulum* were correctly found east of the

predicted hybrid zone and how many were incorrectly found west of the hybrid zone; this was repeated for *L. gentilis*. We then used a Fisher's exact test to examine matches for each clade and each geographic area. Similarly, using the top 10 SNPs with the lowest cline widths at each hybrid zone, we also used Fisher's exact test to understand congruence between GBS data and mtDNA on each side of the two hybrid zones. To further understand the extent of mtDNA differences, we examined sequence divergence and the number and type of amino acid differences among *L. gentilis*, *L. triangulum*, and *L. elapsoides.*

Ecological Niche Modeling Through Time

To understand if aspects of niche estimated using climatic variables have diverged between adjacent species pairs of milksnakes (*L. gentilis* and *L. triangulum*; *L. triangulum* and *L. elapsoides*) we used ecological niche models (ENM) and associated tests. We also predicted the range and changes in area for each taxon given contemporary and Last Glacial Maximum (LGM; 21 Ky) climates and compared this to changes in population size estimates using historical demographic methods (discussed above). We downloaded all localities of *L. triangulum* and *L. elapsoides* from VertNet (http://vertnet.org/), which included all species examined here. After removing samples that were not georeferenced, we recovered 2774 samples. We cropped the remaining individuals to the boundaries of North America included here (see Fig. 1). Using the genetic points sampled in this study, which liberally represent the known ranges of these three taxa, we circumscribed these VertNet samples to identify individuals within the range of each of taxon (*L. gentilis*, *L. triangulum*, *L. elapsoides*). For each taxon that included VertNet samples and localities from genetic data, we further cleaned these data by discarding duplicates and reducing spatial autocorrelation by thinning each species to 200 samples using the R function *thin.max* (https://gist.github.com/danlwarren/271288d5bab45d2da549). We downloaded the 19 bioclimatic variables at 2.5 arcmin resolution for current climates from the CHELSEA global climate data set (Karger et al. 2017) and LGM variables from Brown et al. (2018) and removed all variables correlated with other variables >0.7 to infer ENMs (for details on estimating ENMs see Electronic Supplementary Text S1). The averages of the ENMs for each taxon were hindcasted to LGM variables using the CCSM4 general circulation model projections for the same uncorrelated bioclim variables from current climate data. We then estimated the magnitude of expansion from 21Ky by i) calculating the total area obtained for each climate layer through time given occurrence probabilities taken from the actual location of samples and mean occurrence probabilities and then ii) dividing the total area from current predictions by the total area for LGM predictions.

Using these same data, we quantified contemporary niche similarity among pairs of milksnakes using

methods introduced in Bintanja and Van De Wal (2008) using Schoener's *D* and Hellinger distance *I* (Schoener 1968; Van der Vaart 1998). Estimates of *D* and *I* between adjacent species pairs were calculated and significance of niche identity was derived from 500 random permutations of lineage identity and re-estimation of the ecological niche model (ENM) using maxent (Phillips and Dudik 2008) in the R program ENMTools (Warren et al. 2010). We also used the symmetric background test to produce a null distribution ($n =$ 100 replicates) that more broadly sampled available environments within the range of each taxon. This produces ENM using randomized occurrence points within each lineage (sampling from a radius of 20 km and 1000 points). Therefore, if *D* and *I* from the identity tests were significantly lower than the background test null distribution, then similarity between species is rejected, provided that accessible habitat exists in the region (Warren et al. 2008).

All data, scripts, additional text, and additional figures are included in Supplementary material available on Dryad. Raw genomic data are hosted on the SRA website under project number PRJNA778260.

RESULTS

Data and Geographic Clusters

We generated an average of 2.01×10^6 reads/sample for an average of 41,000 loci/sample using ipyrad. Our assembly with 70% of samples present for each locus retained 3812 loci and 11,076 SNPs for 190 individuals. Final filtering for single biallelic SNPs per locus by eliminating >90% missing loci and individuals missing >70% loci produced a final data set of 144 individuals for 3391 biallelic SNPs with missing data per individual ranging from 17% to 69% (mean = 46%).

All three methods of clustering individuals produced similar geographic groupings as found in Ruane et al. (2014). The lowest BIC value for DAPC and threshold for RMSE for TESS3r generated three groups: a southeastern US group corresponding to *L. elapsoides*, a northern and eastern group corresponding to *L. triangulum*, and a group found west of the Mississippi River corresponding to *L. gentilis* (Fig. 1). We estimated 100% assignment probabilities for each of these three species using DAPC (Fig. S2 of the Supplementary material available on Dryad). The inclusion of a fourth group occurring in southern Texas and northeastern Mexico can be found when increasing cluster numbers by one; this group corresponded to *L. annulata*. Admixture coefficients were similar and significantly correlated for all groups when using TESS3r and SNMF ($\rho = 0.92 - 0.96$; $P < 0.001$; Figs. S3 and S4 of the Supplementary material available on Dryad). Considering different filtering strategies with average missing data per individual, number of individuals, and number of loci ranging from 19% to 48%, 129 to 159, and 137 to 3391, respectively, generated

similar results for DAPC and TESS3r (Figs. S5 and S6 of the Supplementary material available on Dryad). Admixture appears highest at the interface between species pairs. However, at the southern end of the Mississippi River, some admixture occurs among all three taxa (Fig. S7 of the Supplementary material available on Dryad). We calculated F_{ST} between *L. gentilis* and *L. elapsoides* = 0.482, *L. triangulum* and *L. elapsoides* = 0.43, and *L. gentilis* and *L. triangulum* = 0.261. Also, we calculated the following numbers of loci showing strong fixation ($F_{ST} > 0.35$): 120 between *L. triangulum* and *L. elapsoides* and 75 between *L. gentilis* and *L. triangulum*.

Effective migration rates estimated using EEMS showed deviations from IBD at similar boundaries defining these groups using clustering methods (Fig. 1). Low effective migration rates occur in the southeastern United States between *L. triangulum* and *L. elapsoides* and in a large area west of the Mississippi between *L. triangulum* and *L. elapsoides* (Fig. 1).

The ML phylogeny of phased individuals shows 100% bootstrap support for *L. elapsoides*, *L. triangulum*, and *L. gentilis* given individuals assigned to species by DAPC (Fig. 2). A clade representing *L. annulata* received 100% support but was not reciprocally monophyletic when compared to *L. gentilis*. When rooting on *L. elapsoides*, we found a similar topology with the PoMo model showing a sister relationship between *L. gentilis* and *L. annulata* and with *L. triangulum* sister to that clade. Similarly, mtDNA trees showed the same clades and relationships, high bootstrap support ≥99, and failure for *L. annulata* to be distinct from *L. gentilis* (Fig. 2). When comparing individual assignments to each mtDNA clade and GBS clades (or groupings using DAPC for GBS), these relationships were significant ($X^2 = 329.8; P < 2.2 \times 10^{-16}$; Fig. 2). All inconsistencies between mtDNA and GBS clade designations occurred (9%) between *L. gentilis* and *L. triangulum* in an area of admixture in Louisiana centered at the Mississippi River (Fig. S8 of the Supplementary material available on Dryad). For these, genome admixture coefficients poorly support *L. triangulum* (0.33–0.36), indicating admixture with *L. gentilis* and *L. elapsoides* and all having only *L. gentilis* mtDNA.

Our SNAPP species-delimitation results were consistent where Bayes factors supported the four-taxon model > 1000 over the three-taxon model and > 2300 over the two-taxon models among all replicates. This was the same for the doubling and tripling of θ priors which were only 1–2 marginal likelihood values different from the estimated θ. Shuffling individuals between *L. gentilis* and *L. triangulum* performed worse (BF > 1100) when compared to the unshuffled estimates among the three replicate analyses.

Allele Surfing

We found correlation between longitude and heterozygosity in only 160 out of 3391 loci when examining allele surfing as a possibility for spurious groupings for *L. triangulum* and *L. gentilis*. After removing those loci where correlation was due to a single heterozygous or single homozygous population at the end of the range (outlier generating correlation), only three loci that changed heterozygosity (two with a positive slope—increase in heterozygosity with increase in longitude, one with a negative slope) remained. These three loci were not the same as those indicated as important for clustering populations, did not have high F_{ST} values, and did not show narrow clines. Similarly, EEMS plots of genetic diversity over the landscape showed no trends in genetic diversity separating these species (Fig. S9 of the Supplementary material available on Dryad). No analyses suggested that species clusters were due to allele surfing.

Historical Demography

After removing individuals with missing data for these whole-locus estimates of demography, we were left with 41 (82 phased), 59 (118 phased), and 40 (80 phased) individuals for *L. elapsoides*, *L. triangulum*, and *L. gentilis*, respectively. The neural network model was able to classify the six demographic hypotheses with 90% accuracy (Fig. S10 of the Supplementary material available on Dryad). The IMD (isolation–migration with a population-size change) model was selected as the best model with a probability of 99%, indicating a high confidence in this selection. We estimated symmetric migration rates with *L. gentilis* receiving *L. triangulum* at 0.53 individuals/generation (95% CI 0.45–0.64) and with *L. triangulum* receiving *L. gentilis* at 0.59 individuals/generation (95% CI 0.42–0.82; Fig. 3B). Migration rates between *L. gentilis* and *L. elapsoides* were also low given little to no overlap in current range, with *L. elapsoides* as the receiver at 0.39 individuals/generation (95% CI 0.29–0.51) and *L. gentilis* as the receiver at 0.31 individuals/generation (95% CI 0.25–0.39). Where ranges overlap, we estimated *L. triangulum* receiving migrants from *L. elapsoides* at 0.18 individuals/generation (95% CI 0.10–0.26) and *L. elapsoides* receiving *L. triangulum* at 0.13 individuals/generation (95% CI 0.07–0.20). Showing some migration here is also confirmed by having areas of admixture (see results from TESS3r).

Similar to Ruane et al. (2014), we estimated divergence times during the Pleistocene and Pliocene for the three Nearctic milksnake taxa, with divergence of *L. elapsoides* from *L. gentilis* and *L. triangulum* at 4.42 My (95% CI 3.25–5.56 My) and between *L. gentilis* and *L. triangulum* at 2.51 My (1.44–3.62 My; Fig. 3C). All species experienced expansion in population size—increasing by 63–71 times (Fig. 3D). These events occurred at similar times for all species (0.903–1.08 My; Fig. 3E), roughly at the mid-Pleistocene Transition (Bintanja and Van De Wal 2008).

Influences on Population Structure

For all four taxa, the first two genetic PCoA axes were predicted using ANN with geographic spatial, environmental, elevational, and barrier variables at 74.5 and 87.3% (SD = 3.3–6.7%) accuracy. Accuracy declined to 64% by the third axis of genetic variation (Fig. 4). For the first two axes of genetic variation, variable importance >50% was estimated for the following nonspatial variables: the Mississippi River, elevation, precipitation of driest month, mean diurnal range, and precipitation of warmest quarter. When controlling for space and using RDA, a significant effect ($P < 0.02$) on genetic structure was found for mean diurnal range, isothermality, max temperature of warmest month, precipitation of wettest quarter, the Great Plains, and the Mississippi River, which isolates *L. elapsoides* to the east. When examining the two most closely related taxa, *L. triangulum* and *L. gentilis*, we obtained 89% and 70.9% (SD = 2.7 and 4.5%) accuracy on the first two axes using ANN. Accuracy declined to 19% by the third PCoA axis. Nonspatial variable importance > 50% was found using the first two axes of genetic variation for elevation, mean temperature of wettest quarter, precipitation of wettest month, and precipitation of warmest quarter. Controlling for geographic spatial variables, RDA showed significance for elevation, mean temperature of wettest quarter, precipitation of wettest month, and precipitation of warmest quarter. The Mississippi River and boundary of the Great Plains did not affect lineage structure between *L. triangulum* and *L. gentilis*.

Clines

Using admixture proportions and geographic distance between *L. triangulum* and *L. gentilis*, we show support for a model with no tails (ΔAICc = 3.97–46.8), though centers and widths were similar across all models. Median cline widths were 350 km (min = 201, max = 400), representing 10.48% of the total distance of both parental species with the cline center for *L. triangulum* and *L. gentilis* predicted at 14.49 (min = −31; max = 74; Fig. 5). Support was highest for the preferred environmental cline model with no tails for *L. triangulum* and *L. gentilis* (ΔAICc = 4.4–17.1), predicting median widths at 1.94 (min = 0.72, max = 3.44) representing 7.6% of the total environmental width of the parental species. For *L. triangulum* and *L. elapsoides*, we showed support for a model with no tails (ΔAICc = 3.56–8.36) with a cline width of 248 km (min = 119 km, max = 396 km; Fig. 5), which represented 12.1% of the parental species and a cline center at -13.2 (min = −53, max = 28.61). For *L. triangulum* and *L. elapsoides*, environmental clines also supported the "mirrored tail" model (ΔAICc = 6.51–15.60) with a width of 3.31 (min = 0.46; ax = 6.66) representing 23% of the total environmental width of the parental species. Estimates of widths of zones of low migration between lineages using EEMS migration indicate that these are likely highly variable over the

range where taxon-pairs connect. For example, estimates of low-migration areas range from 91 km to 308 km between *L. gentilis* and *L. triangulum*, and between 74 km and 255 km between *L. triangulum* and *L. elapsoides*. We note that in some areas the latter taxon pair may coexist in broad areas with no hybridization (Williams 1988), therefore estimates of width in some areas may be inaccurate given our clinal predictions.

We predicted neutral widths at 200 km for 1 km lifetime dispersal rates and 803 km for 4 km lifetime dispersal rates for clines originating at the end of the LGM. For *L. triangulum* and *L. gentilis*, we estimated five loci fixed in the tails of the distributions of the parental taxa with cline widths below 200 km with cline centers within 200 km of interpolated estimate. These cline widths ranged from 53 km to 191 km (median = 153 km; Fig. 6). We found 30 loci with cline widths below 803 km also within 200 km of the center; we estimated ranges of width from 105 km to 740 km (median 343 km). For the more deeply diverged *L. triangulum* and *L. elapsoides*, where a clear cline across their ranges may not be constant, we found 40 loci with cline widths below 200 km with width ranges from 28 km to 199 km (median 117 km). For a threshold of 803 km, we found 88 loci with a range of 28–786 km (median = 237 km; Fig. 5). Rerunning both TESS3r and DAPC with just 9 loci falling below a neutral cline width for *L. triangulum* and *L. gentilis* and 40 loci between *L. triangulum* and *L. elapsoides* generated the same spatial genetic structure using all loci (Fig. S11 of the Supplementary material available on Dryad). The highest F_{ST} values for each locus (>0.9) were always associated with those having low cline widths (Fig. S12 of the Supplementary material available on Dryad).

mtDNA Phylogenetic and Spatial Structure

Both AIC and BIC chose the HKY+F+R2 model of substitution for the mtDNA. The trees were similar to those in Ruane (2015) showing 100% support for three geographic clades corresponding to *L. gentilis*, *L. triangulum*, and *L. elapsoide*s. Here, *L. annulata* does not form a clade distinct from *L. gentilis*. Significant spatial congruence between mtDNA and GBS groupings and hybrid zone estimates were found for pairs at the following hybrid zones: *L. triangulum/L. gentilis* and *L. triangulum/L. elapsoides* ($P < 0.00001$; Fig. S13 of the Supplementary material available on Dryad). Similarly, the top 10 SNPs with the lowest cline widths were also spatially congruent with mtDNA for these taxon pairs ($P < 3 \times 10^{-7}$). Discordances only appear in the lower Mississippi in Louisiana, which is predicted to be an area of admixture from GBS data alone (Figs. S7 and S8 of the Supplementary material available on Dryad). There were 13 amino acid substitutions in cytochrome b between *L. triangulum* and *L. gentilis* resulting in five neutral polar to hydrophobic differences and one hydroaromatic to hydroaliphatic change. The average sequence distance between these species was 6.62% (sd = 0.004) compared to the average within-species distances of 0.5% (sd = 0.5%) and 0.9% (sd
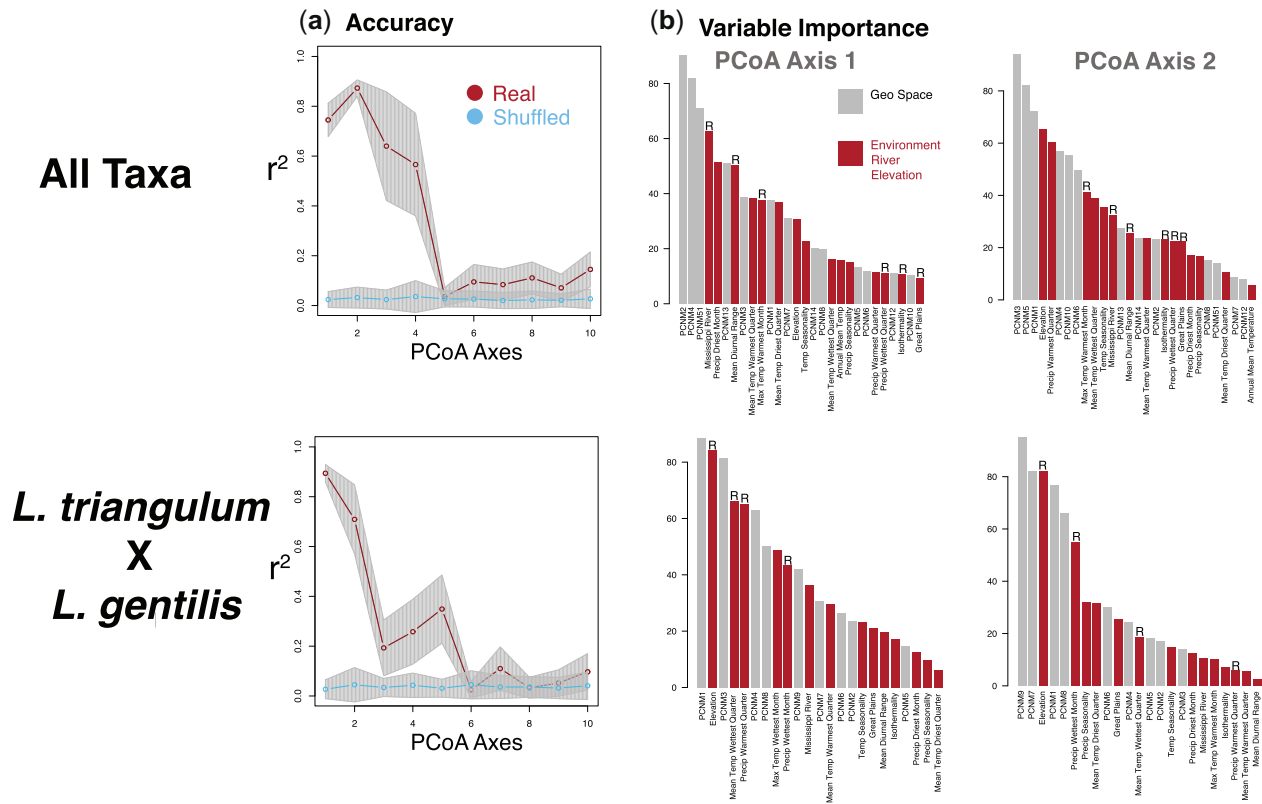
FIGURE 4.   a) Artificial neural networks (ANN) showing predicted accuracy (with standard deviation over 100 replicates in gray) of spatial, biogeographic barriers (Mississippi River and Great Plains), and environmental models for predicting the first 10 principal coordinates (PC) axes against a random shuffling of predictor variables for four Nearctic milksnake taxa (*Lampropeltis*) and then for *L. gentilis* × *L. triangulum*. b) Importance of spatial (gray) and environmental (red) variables estimated from using ANN. The letter "R" above each variable importance column indicates significance at $P < 0.05$ using RDA.

=0.6%) for *L. triangulum* and *L. gentilis*, respectively. There were nine amino acid differences in cytochrome b between *L. elapsoides* and *L. triangulum* with two neutral polar to hydrophobic changes and one hydroaromatic to hydroaliphatic change. The average percentage of sequence differences between *L. triangulum* + *L. gentilis* and *L. elapsoides* was 10.5% (sd =0.6%) and within *L. elapsoides* was 0.6% (sd =0.5%).

Ecological Niche Modeling Predictions

Predicted areas for the three Nearctic species were similar to current range maps (Powell et al. 2016) with *L. gentilis* occupying drier areas in western North America, *L. triangulum* occurring in the forested regions of eastern North America, and *L. elapsoides* occurring in the forested regions of the southeastern United States (Fig. 7). The Linear, Quadratic, and Hinge models were favored for *L. gentilis* and *L. triangulum*, and the same models plus Threshold for *L. elapsoides*. For each model, we found area under the curve (AUC) values ranged from 0.91 to 0.99, sensitivity estimates ranging from 91.0 to 96.5, and specificity ranged from 80.1 to 95.87 for the final maxent model for each taxon.

Ancestral areas at the LGM predict compression of all three species overlapping in the Gulf Coast of the United States (Fig. 7). Expansion of area from this refugium in the LGM to contemporary climates ranged in magnitude from 2.11 to 31.09 for *L. gentilis*, 2.29 to 4.57 for *L. triangulum*, and 0.64 to 1.62 for *L. elapsoides*.

Niche equivalency tests were significant among all tested species pairs: *L. gentilis*—*L. triangulum*: D statistic =0.25, I statistic =0.52, $P=0.0099$; *L. triangulum*—*L. elapsoides*: D statistic =0.29, I statistic =0.53, $P=0.0099$. Symmetric background tests were significant for *L. gentilis*—*L. triangulum* (D statistic =0.22, I statistic =0.47, $P=0.0099$) and *L. triangulum*—*L. elapsoides* (D statistic =0.26, I statistic =0.49, $P=0.0099$).

DISCUSSION

Biogeography

We show support for large-scale environmental effects, biogeographic barriers, and geographic distance on phylogeographic structure in independently evolving Nearctic milksnakes. These species likely formed in parapatry and where ranges overlap between species, we detect gene flow throughout the Pleistocene. With older divergence times, we detect less gene flow and a greater number of alleles failing to traverse clinal
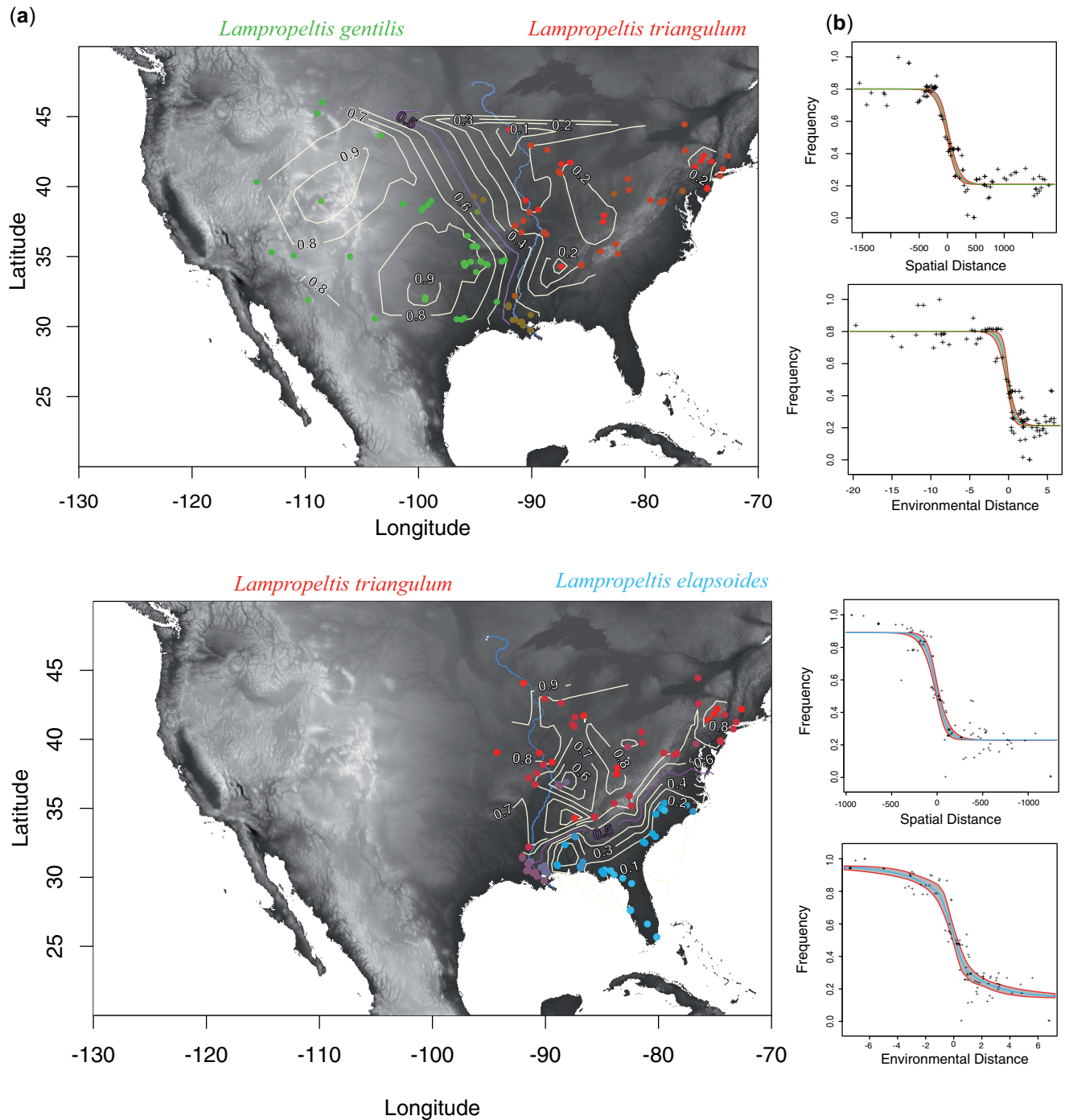
FIGURE 5.   a) Interpolated contour lines showing estimates of admixture between species-pair contact zones (numbers on white lines) showing the centers (purple) of the hybrid zones in three Nearctic milksnakes (*Lampropeltis*). Pure parental-colored points are represented as red (*L. triangulum*), green (*L. gentilis*), and blue (*L. elapsoides*) with intermediate colors showing higher admixture coefficients. The Mississippi River is represented in blue. b) Gaussian cline predictions using admixture estimates for both spatial and environmental distances for each species-pair comparison.

areas. This demonstrates that the degree of reproductive isolation is related to the age of divergence. Our results also indicate that three species of milksnakes examined here are currently experiencing different contemporary environments but were compressed into the same glacial refugium reflecting parallel changes in historical demography.

Often, genetic structure in widespread species complexes is thought to be driven by prominent biogeographic barriers, particularly in eastern North America (Avise et al. 1992; Bierne et al. 2013). Phylogeographic structure and variation within the milksnakes formed via combined effects of a hard allopatric barrier in the form of the Mississippi River,
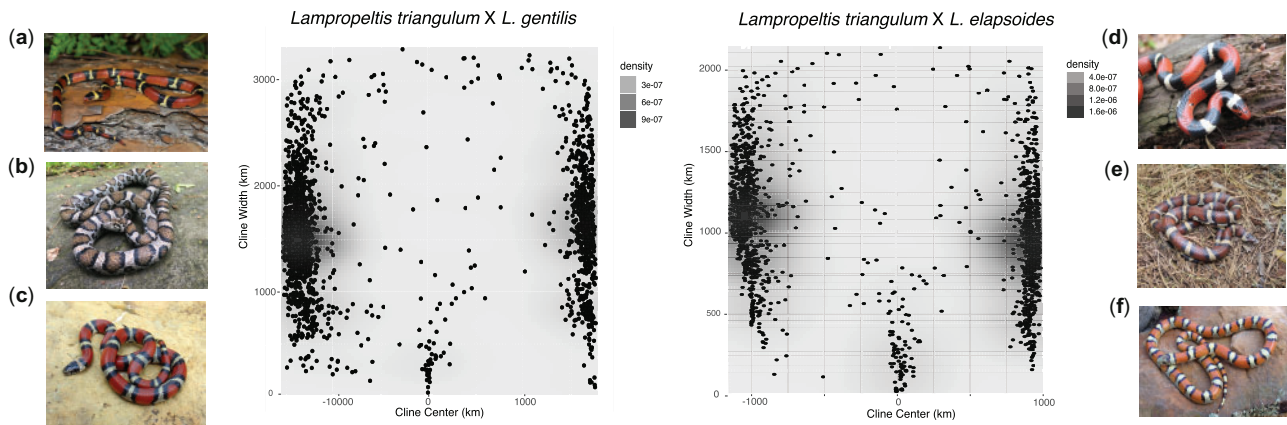
FIGURE 6.   Graphs showing estimated cline widths and cline centers for all loci between species-pair comparisons for three Nearctic milksnakes (*Lampropeltis*). Loci with cline widths and centers near the origin of the graph were generated by nonneutral clinal processes. Photos: a) *L. elapsoides*—Mississippi (A. Meier), b) *L. triangulum*—New York (F. Burbrink), c) *L. gentilis*—Oklahoma (D. Shepard), d) *L. elapsoides*—Alabama (S. Ruane), e) *L. triangulum*—New Jersey (T. Huang), f) *L. gentilis*—Montana (D. Shepard).
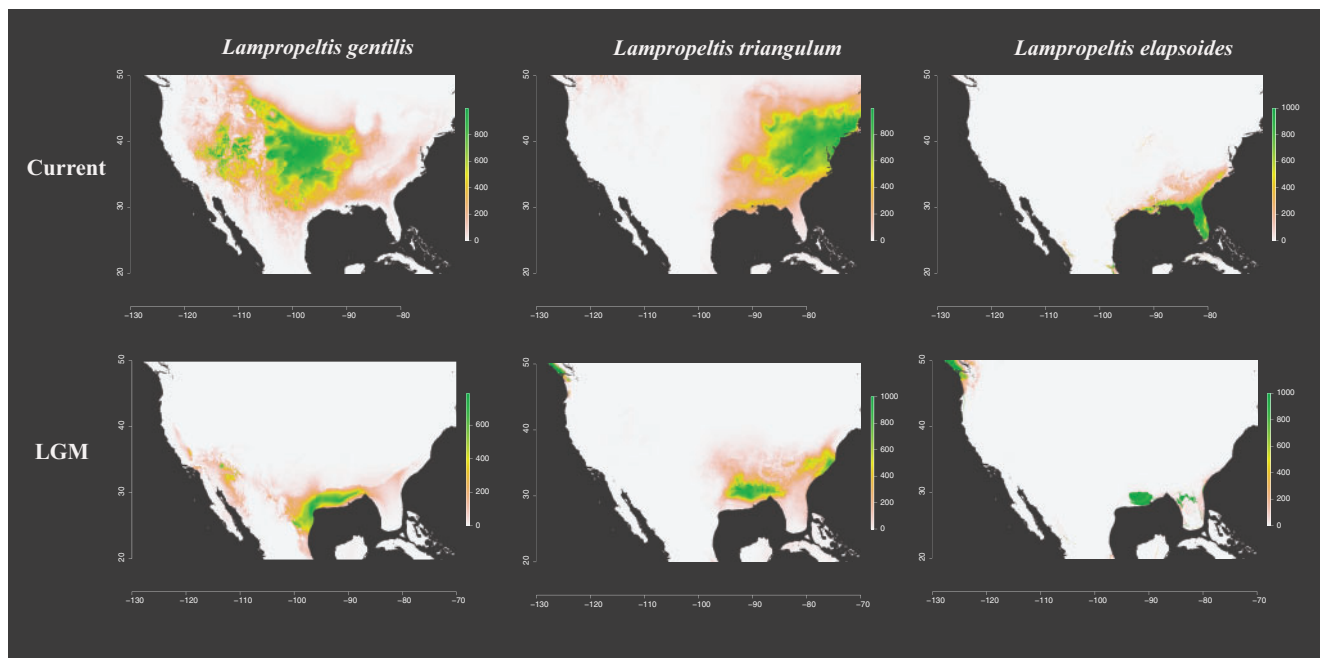
FIGURE 7.   Habitat suitability predicted under current climate and the Last Glacial Maximum (LGM) over North America for three Nearctic milksnakes. Colors represent suitability based on bioclimatic variables from highest (green) to unsuitable (white).

limiting only the western extent of the range for *Lampropeltis elapsoides*, climate defining the differences among species, and space-associated genetic differences within and among taxa. *Lampropeltis elapsoides* and *L. triangulum* appear to be isolated by climate in the southeastern United States (Fig. 7) rather than a distinct biogeographic barrier. In most parts of their range, *L. elapsoides* prefers pine forests, but occasionally will occur in deciduous hardwoods sympatrically with *L. triangulum* in northern areas of their range and showing limited or no gene flow between the two (Williams 1988; Armstrong et al. 2001).

In the west, forests of the Eastern Nearctic decline in the prairie savannahs, with long and short grass prairies giving rise to the Great Plains (Hanberry 2019). However, the actual boundary of the division between ecoregions is not currently a factor isolating the ranges of *L. triangulum* and *L. gentilis*. Rather, changes in elevation, temperature and precipitation (positive longitudinal increases in precipitation) that were not directly correlated with the boundary of the GP have a greater effect on structuring these species (Figs. 1, 4, and 7). This transition between forested areas and grasslands represent major turnover in herpetological community structure (Costa et al. 2008). There are ~80 species of reptiles in the ENA with a range concluding at or near the GP, and another 40 species from the GP that fail to cross into forested ecoregions of the ENA (Powell et al. 2016).

A study on copperheads (*Agkistrodon contortrix* complex) showed divergence near the ENA/GP interface with a similar location for the hybrid zone (Burbrink and Guiher 2015). Similarly, some mammals and birds show comparable phylogeographic structure at these suture zones associated with the GP (Remington 1968; Swenson and Howard 2005; Swenson 2006; Reding et al. 2012, 2021). However, the current boundary of the GP may not be the main force generating deep structure in many of these taxa. Furthermore, the boundary of these habitats was likely not static through time. The standard narrative theorizes that divergence and isolation in the Pleistocene and secondary contact in the GP may account for the current structure along these suture zones (Hall and Kelson 1959; Barton and Hewitt 1985; Reding et al. 2021). For the milksnakes, we find that at least during the Last Glacial Maximum niche modeling predictions do not support extreme west and east isolation among lineages but rather continued contact near the Gulf Coast. We provide evidence for continuous gene flow throughout the Pleistocene indicating that strict allopatry and secondary contact east of the GP cannot account for current genetic and distributional structure (Fig. 3). This rejects a hypothesis that long-term allopatry was a driving force of divergence for these species and instead shows support for the MIM model (He et al. 2019), indicating only partial isolation and connection through time. It is possible then that a single process of spatial and temporal isolation and subsequent demographic change cannot alone account for the phylogeographic structure of most of the physiologically unique vertebrates diverging at the intersection of the Eastern Nearctic and Great Plains.

In the ENA, genetic structure when including all three milksnake taxa can be predicted by the Mississippi River, ecoregion, elevation, and Pleistocene climate variables. The Mississippi River has a major effect on the genetic structure of many unrelated organisms and has been indicated as important for multiple species of snakes (Burbrink et al. 2000, 2021; Soltis et al. 2006; Zellmer et al. 2012; Wieringa et al. 2020). In this system, it serves to only limit the western range of *L. elapsoides* but not the divergence between *L. gentilis* and *L. triangulum* (Fig. 1). It is possible that the initial divergence of *L. elapsoides* relative to other milksnakes occurred in the southeastern United States, or more specifically the Florida peninsula as demonstrated for other species of snakes with similar ranges (Burbrink et al. 2000, 2008; Fontanella et al. 2008; Burbrink and Guiher 2015). *Lampropeltis elapsoides* has likely expanded its range given demographic predictions and locations as far north as Tennessee, Kentucky, and Virginia (Armstrong et al. 2001; Roble et al. 2007; Fig. 1); alternatively, these areas may represent relict populations following larger extirpation events. Results from our hindcast niche models at the LGM and estimates of admixture suggest that these three taxa shared genes recently and in the past (Fig. 7; Figs. S7 and S13 of the Supplementary material available on Dryad).

Migration

Despite divergences in the late Miocene between *L. elapsoides* and all other milksnake taxa, and divergences in the early-to-mid-Pleistocene between *L. gentilis* and *L. triangulum*, some gene flow still occurs between all three taxa where ranges overlap. Given evidence from clustering methods, migration over space, tree structure, and coalescent estimates, we demonstrate that these lineages represent real entities and are not the spurious predictions resulting from IBD (Figs. 1, 2, and 4). All three taxa overlap mainly along the Gulf Coast in Louisiana, an area where their ranges were concentrated in the same refugia along the US Gulf Coast during the LGM (Fig. 7). Here the greatest admixture among taxa and mitochondrial capture in the southern portion of the range occurs closer to the Mississippi River and outside of the GP (Fig. 1, Fig. S7 of the Supplementary material available on Dryad). It is possible that noted difficulty assigning individuals to the former subspecies occurring in this area, such as *L. t. amaura*, is partially the result of historical and contemporary admixture in this region (Williams 1988). This area of admixture has been identified using genomic data for other species of snakes (Burbrink et al. 2021) and bears further examination to understand potential mixed-genomic interactions within the numerous species pairs showing divergences at the Mississippi River (Borcard and Legendre 2002; Pyron and Burbrink 2009; Brandley et al. 2010; Wieringa et al. 2020).

Clines between *L. elapsoides*/*L. triangulum* and *L. gentilis*/*L. triangulum* were estimated to be large (>200 km). Our predictions from EEMS suggest that areas of low migration associated with these clines likely change width along the hybrid zone from narrow (74 km) to wide (208 km; Figs. 1 and 7). Cline widths were narrower for environment when compared to space and these clines are closely associated with the intersection of ranges for each of these three species based on climate differences. This indicates that the environment may be constraining interactions between taxa and occurrence may be limited in this region, particularly in the eastern taxa (see distributional maps in Williams 1988). We underscore that our estimates of width are coarse and likely represent mean estimates across the entire cline, necessitating future studies that use straight line transects through these zones of contact to better understand interactions here.

The younger species pair, *L. gentilis* and *L. triangulum*, meet east of the boundary between the grasslands of the Great Plains and the forested Eastern Nearctic and likely diverged prior to 2 Mya, showing migration on average from 0.53 to 0.59 migrants/generation in each direction. Among many nonmodel organisms, there is a large range of interspecific introgression (Baack and Rieseberg 2007; Chatfield et al. 2010; Harrison and Larson 2014; Payseur and Rieseberg 2016; Martin et al. 2019) and perhaps estimating gene flow with the assumption of neutrality should generally be questioned. At one extreme, we have

identified 5 loci that do not traverse the predicted neutral cline of 200 km at the boundary of the ecoregions and as few as 9 loci can accurately cluster individuals across geographic space as well as the full data set (Fig. 6; Fig. S11 of the Supplementary material available on Dryad). Because these loci are limited to the samples and geographic positions used here with some individuals missing data, it is likely that cline widths could be narrower for many more loci with $F_{ST} > 0.7$ (Fig. S12 of the Supplementary material available on Dryad); up to 30 loci show nonneutral cline widths given larger cline estimates using total admixture. These candidate loci with high F_{ST} values serve as a starting point for examining functional differences between these species and potential negative allelic interactions within contact zones.

When comparing the overlap between the nonsister *L. triangulum* and *L. elapsoides*, we show lower rates of migration/generation (0.13–0.18 migrants/generation) with 40 loci falling well below the spatial threshold for neutrality (Fig. 6). While these taxa may exist sympatrically where ranges overlap, establishing a cline may be difficult if hybridization occurs sporadically and inconsistently across this region.

Historical Demography

Introgression in temperate regions may be common where ranges are cyclically altered by Pleistocene glacial cycles. In North America, populations are thought to have been compressed and isolated in refugia at glacial maxima and then reconnected upon climate amelioration (Harrison 1993; Hewitt 2004; Waltari et al. 2007). Historical demography of vertebrates in eastern North America in response to changing glacial cycles has been examined extensively. Most snakes examined so far have shown positive and synchronous changes related to contracting glaciers (Burbrink et al. 2016), although previous work on milksnake species from North, Central and South America have shown variable responses to Pleistocene climates (Ruane et al. 2015). While species distributed across the Nearctic are often predicted to have unique refugia (Waltari et al. 2007), our results show all three focal Nearctic species co-occurred in the same refugium at the US Gulf Coast, with *L. gentilis* and *L. triangulum* both expanding out of this refugium and colonizing the western and eastern areas of the United States, respectively (Fig. 6). Our historical demography models are congruent with the ENM predictions and support population expansion on a massive scale (63- to 71-fold increase; Fig. 3). However, demographic expansion likely occurred coetaneously at ~1 Mya. If we assume that these expansions occurred at similar times, then both taxa likely maintained physical contact since the mid-Pleistocene. Given this ancient age of contact and that parental species remain unique, this provides some support that these taxa have existed for more than 1,000,000 years in a state of partial reproductive isolation (Servedio and Hermisson 2020).

The interaction between these species and adapted traits within the hybrid zone that resist hybridization and promote genomic divergence bears further exploration.

Future directions for these and other organisms showing similar genetic discontinuities in the southeastern United States and near the Great Plains should address if the same environmental processes throughout the Pleistocene have generated similar phylogeographic structure. Additionally, examination of whole genomic data for many individuals at the hybrid zones will help determine the function of poorly introgressing loci and if they are located in recombination cold spots and thus resist migration (Nosil et al. 2009; Cruickshank and Hahn 2014; Booker et al. 2020). Furthermore, estimates of the degree of linkage disequilibrium here spanning the range from pure parental taxa to hybrids will determine if selection against various allelic combination occurs. This system should provide key information on the argument regarding the origins of alleles as genomic islands or selective sweeps and also account for interaction of alleles in expanding populations among interacting lineages (MacPherson et al. 2021).

Taxonomic Conclusions

Given the timing of origin, niche divergence, morphological differences (Ruane 2015), general phylogenetic agreement between mtDNA and nDNA genomes, and lack of gene flow for portions of the genome (Figs. 1–3 and 7; Figs. S8 and S13 of the Supplementary material available on Dryad), we suggest that *L. triangulum* and *L. gentilis* remain recognized as unique species. Greater sampling will be needed to further address the status of *L. annulata*. Other authors have shown some differences in the number of bands or saddles (Williams 1988) geographically associated with *L. gentilis*, *L. triangulum*, and *L. elapsoides* as defined in our study, though additional work is needed to better understand how morphology changes over space and at the boundaries of zones of contact. These lineages have maintained their identity despite consistent gene-flow-through time and being compressed into overlapping refugial areas during the LGM (Fig. 7). Roux et al. (2016), Jackson et al. (2017), and Leaché et al. (2019) have examined some of the following metrics to predict if candidate lineages should be considered species given neutral gene coalescent estimates: i) individual estimates of species divergence time/population size ($2\tau/\theta > 1$), ii) absolute divergence time (10^4), and iii) maximum migration rates ($M = N_m < 1$). Values below those thresholds for all three metrics were attained for all species comparisons here (Fig. 3). Despite the presence of a hybrid zone for *L. triangulum* and *L. gentilis*, the identity of parental species is still discoverable and has remained unaffected for >1,000,000 generations with low levels of migration/generation. It therefore stands to reason that these species remained in partial reproductive isolation over a long period of time (Gagnaire et al. 2013; Servedio and Hermisson 2020).

Under the general lineage species concept and evolutionary species criterion, we suggest that these lineages have retained their unique trajectories given differences in niche and reduced gene flow and therefore be considered distinct species (Simpson 1951; de Queiroz 2007).

Previous studies examining population structure using only a portion of our previously published Sanger data (Ruane et al. 2014) concluded that divergence between these two lineages was spurious, likely the product of IBD, and that continuous clines were arbitrarily dissected (Chambers and Hillis 2020). Here with genome-scale data and much greater individual sampling, we show that IBD did not produce false lineages. Furthermore, methods examining selection on loci and those that relate neutral estimates of migration to divergence time all suggest the presence of distinct species. Taxonomic inflation is undesirable; however, the flip side of the coin of underestimating diversity is also problematic. Consequently, revising established taxonomies by eliminating taxa without supporting data, analyses, or theory have known negative downstream effects on estimating diversification, understanding basic ecology and devising conservation strategies (May 1990; Prance 1995; Caye et al. 2016; Cusimano and Renner 2010; Davies et al. 2012; Rangel et al. 2015 but see Morrison et al. 2009 for alternative views).

Given gene flow, some researchers may prefer a taxonomy where subspecies represent historical entities (Hillis 2020), indicating prospectively that these lineages are on their way to forming species (with reduced gene flow) or will collapse (increased gene flow). If species are defined ontologically as spatio-temporal individuals with fuzzy boundaries and not classes (Ghiselin 1974; Hull 1976; Mishler and Donoghue 1982; Frost and Kluge 1994; Mayden 2002; Velasco 2008; Reydon 2009), then defining subspecies prospectively has already met the basic criterion of being species. That is, defining subspecies is redundant with the species category in that spatio-temporal lineages have been discovered regardless of what gene flow or lack of gene flow will do to those lineages in the future. We advocate that these lineages therefore retain the rank of species and be revised in the future if collapse via hybridization eliminates these independently evolving species.

REFERENCES

Abbott R., Albach D., Ansell S., Arntzen J.W., Baird S.J.E., Bierne N., Boughman J., Brelsford A., Buerkle C.A., Buggs R., Butlin R.K., Dieckmann U., Eroukhmanoff F., Grill A., Cahan S.H., Hermansen J.S., Hewitt G., Hudson A.G., Jiggins C., Jones J., Keller B., Marczewski T., Mallet J., Martinez-Rodriguez P., Möst M., Mullen S., Nichols R., Nolte A.W., Parisod C., Pfennig K., Rice A.M., Ritchie M.G., Seifert B., Smadja C.M., Stelkens R., Szymura J.M., Väinölä R., Wolf J.B.W., Zinner D. 2013. Hybridization and speciation. J. Evol. Biol. 26:229–246.

Abe-Ouchi A., Saito F., Kawamura K., Raymo M.E., Okuno J., Takahashi K., Blatter H. 2013. Insolation-driven 100,000-year glacial cycles and hysteresis of ice-sheet volume. Nature 500:190–193.

Ackermann R.R., Bishop J.M. 2010. Morphological and molecualr evidence reveals recent hybridization between gorilla taxa. Evolution (NY) 64:271–290.

Akima H., Gebhard A., Petzoldt T., Maechler M. 2016. Interpolation of irregularly and regularly spaced data [R package akima version 0.6-2.1]. Available from: https://cran.r-project.org/package=akima.

Armstrong M.P., Frymire D., Zimmerer E.J. 2001. Analysis of sympatric populations of *Lampropeltis triangulum syspila* and *Lampropeltis triangulum elapsoides*, in western Kentucky and adjacent Tennessee with relation to the taxonomic status of the Scarlet Kingsnake. J. Herpetol. 35:688–693.

Avise J.C. 1992. Molecular population-structure and the biogeographic history of a regional fauna-a case-history with lessons for conservation biology. Oikos 63:62–76.

Avise J.C. 2000. Phylogeography: the history and formation of species. Cambridge, MA: Harvard University Press.

Avise J.C., Alisauskas R.T., Nelson W.S., Ankney C.D. 1992. Matriarchal population genetic-structure in an avian species with female natal philopatry. Evolution (NY) 46:1084–1096.

Axelrod D.I. 1985. Rise of the grassland biome, central North America. Bot. Rev. 51:163–201.

Baack E.J., Rieseberg L.H. 2007. A genomic view of introgression and hybrid speciation. Curr. Opin. Genet. Dev. 17:513–518.

Bailey R.G. 1995. Description of the ecoregions of the United States. USDA Forest Service.

Barton H.H., Gale K. 1993. Genetic analysis of hybrid zones. Hybrid zones and the evolutionary process. New York: Oxford University Press. p. 13–45.

Barton N.H., Hewitt G.M. 1985. Analysis of hybrid zones. Annu. Rev. Ecol. Syst. 16:113–148.

Bierne N., Gagnaire P.A., David P. 2013. The geography of introgression in a patchy environment and the thorn in the side of ecological speciation. Curr. Zool. 59:72–86.

Bintanja R., Van De Wal R.S.W. 2008. North American ice-sheet dynamics and the onset of 100,000-year glacial cycles. Nature 454:869–872.

Booker T.R., Yeaman S., Whitlock M.C. 2020. Variation in recombination rate affects detection of outliers in genome scans under neutrality. Mol. Ecol. 29:4274–4279.

Borcard D., Legendre P. 2002. All-scale spatial analysis of ecological data by means of principal coordinates of neighbour matrices. Ecol. Model. 153:51–68.

Bouckaert R., Heled J., Kühnert D., Vaughan T., Wu C.-H., Xie D., Suchard M.A., Rambaut A., Drummond A.J. 2014. BEAST 2: a software platform for Bayesian evolutionary analysis. PLoS Comput. Biol. 10:e1003537.

Brandley M.C., Guiher T.J., Pyron R.A., Winne C.T.T., Burbrink F.T. 2010. Does dispersal across an aquatic geographic barrier obscure phylogeographic structure in the diamond-backed watersnake (*Nerodia rhombifer*)? Mol. Phylogenet. Evol. 57:552–560.

Brown J.L., Hill D.J., Dolan A.M., Carnaval A.C., Haywood A.M. 2018. PaleoClim, high spatial resolution paleoclimate surfaces for global land areas. Sci. Data. 5:180254.

Bryant D., Bouckaert R., Felsenstein J., Rosenberg N.A., RoyChoudhury A. 2012. Inferring species trees directly from biallelic genetic markers: bypassing gene trees in a full coalescent analysis. Mol. Biol. Evol. 29:1917–1932.

Burbrink F.T., Chan Y.L., Myers E.A., Ruane S., Smith B.T., Hickerson M.J. 2016. Asynchronous demographic responses to Pleistocene climate change in Eastern Nearctic vertebrates. Ecol. Lett. 19:1457–1467.

Burbrink F.T., Fontanella F., Pyron R.A., Guiher T.J., Jimenez C., Alexander Pyron R. 2008. Phylogeography across a continent: the evolutionary and demographic history of the North American racer (Serpentes: Colubridae: *Coluber constrictor*). Mol. Phylogenet. Evol. 47:274–288.

Burbrink F.T., Gehara M. 2018. The biogeography of deep time phylogenetic reticulation. Syst. Biol. 67:743–755.

Burbrink F.T., Gehara M., McKelvy A.D., Myers E.A. 2021. Resolving spatial complexities of hybridization in the context of the gray zone of speciation in North American ratsnakes (*Pantherophis obsoletus* complex). Evolution 75: 260–277.

Burbrink F.T., Grazziotin F.G., Pyron R.A., Cundall D., Donnellan S., Irish F., Keogh J.S., Kraus F., Murphy R.W., Noonan B., Raxworthy C.J., Ruane S., Lemmon A.R., Lemmon E.M., Zaher H. 2020. Interrogating genomic-scale data for Squamata (lizards, snakes, and amphisbaenians) shows no support for key traditional morphological relationships. Syst. Biol. 69:502–520.

Burbrink F.T., Guiher T.J. 2015. Considering gene flow when using coalescent methods to delimit lineages of North American pitvipers of the genus *Agkistrodon*. Zool. J. Linn. Soc. 173: 505–526.

Burbrink F.T., Lawson R., Slowinski J.B. 2000. Mitochondrial DNA phylogeography of the polytypic North American rat snake (*Elaphe obsoleta*): a critique of the subspecies concept. Evolution (NY) 54:2107–2118.

Burbrink F.T., Myers E.A. 2015. Both traits and phylogenetic history influence community structure in snakes over steep environmental gradients. Ecography (Cop.) 38:1036–1048.

Caye K., Deist T.M., Martins H., Michel O., François O. 2016. TESS3: fast inference of spatial population structure and genome scans for selection. Mol. Ecol. Resour. 16:540–548.

Chambers E.A., Hillis D.M. 2020. The multispecies coalescent over-splits species in the case of geographically widespread taxa. Syst. Biol. 69:184–193.

Chatfield M.W., Kozak K.H., Fitzpatrick B.M., Tucker P.K. 2010. Patterns of differential introgression in a salamander hybrid zone: inferences from genetic data and ecological niche modelling. Mol. Ecol. 19:4265–4282.

Chen X., Lemmon A.R., Lemmon E.M., Pyron R.A., Burbrink F.T. 2017. Using phylogenomics to understand the link between biogeographic origins and regional diversification in ratsnakes. Mol. Phylogenet. Evol. 111:206–218.

Chollet F. 2015. Keras. Available from: https://github.com/fchollet/keras.

Costa G.C., Wolfe C., Shepard D.B., Caldwell J.P., Vitt L.J. 2008. Detecting the influence of climatic variables on species distributions: a test using GIS niche-based models along a steep longitudinal environmental gradient. J. Biogeogr. 35:637–646.

Coyne J.A., Orr H.A. 2004. Speciation. Sunderland: Sinnauer Associates Inc.

Cruickshank T.E., Hahn M.W. 2014. Reanalysis suggests that genomic islands of speciation are due to reduced diversity, not reduced gene flow. Mol. Ecol. 23:3133–3157.

Cusimano N., Renner S.S. 2010. Slowdowns in diversification rates from real phylogenies may not be real. Syst. Biol. 59:458–464.

Davies T.J., Kraft N.J.B., Salamin N., Wolkovich E.M. 2012. Incompletely resolved phylogenetic trees inflate estimates of phylogenetic conservatism. Ecology 93:242–247.

Derryberry E.P., Derryberry G.E., Maley J.M., Brumfield R.T. 2014. hzar: hybrid zone analysis using an R software package. Mol. Ecol. Resour. 14:652–663.

de Queiroz K. 2007. Species concepts and species delimitation. Syst. Biol. 56:879–886.

Diniz-Filho J.A.F., Soares T.N., Lima J.S., Dobrovolski R., Landeiro V.L., Telles M.P.D.C., Rangel T.F., Bini L.M. 2013. Mantel test in population genetics. Genet. Mol. Biol. 36:475–485.

Dixon P. 2003. VEGAN, a package of R functions for community ecology. J. Veg. Sci. 14:927–930.

Dobzhansky T. 1937. Genetics and the origins of species. New York: Columbia University Press.

Dong F., Hung C.-M., Yang X.-J. 2020. Secondary contact after allopatric divergence explains avian speciation and high species diversity in the Himalayan-Hengduan Mountains. Mol. Phylogenet. Evol. 143:106671.

Drummond A.J., Rambaut A. 2007. BEAST: Bayesian evolutionary analysis by sampling trees. Bmc Evol. Biol. 7.

Eaton D.A.R., Overcast I. 2020. ipyrad: interactive assembly and analysis of RADseq datasets. Bioinformatics 36:2592–2594.

Edwards S., Hopkins R., Mallet J. 2020. Speciation. In: Scheiner S., Mindell D., editors. The theory of evolution. Chicago: University of Chicago Press. p. 296–318.

Elshire R.J., Glaubitz J.C., Sun Q., Poland J.A., Kawamoto K., Buckler E.S., Mitchell S.E. 2011. A robust, simple genotyping-by-sequencing (GBS) approach for high diversity species. PLoS One. 6:e19379.

Endler J.A. 1977. Geographic variation, speciation, and clines. Princeton (NJ): Princeton University Press.

Ernst C.H., Ernst E.M. 2003. Snakes of the United States and Canada. Washington, D.C.: Smithsonian Books.

Excoffier L., Ray N. 2008. Surfing during population expansions promotes genetic revolutions and structuration. Trends Ecol. Evol. 23:347–351.

Fisher R.A. 1930. The genetical theory of natural selection. Oxford: Clarendon Press.

Fitch H.S. 1999. A Kansas snake community: composition and change of 50 years. Malabar, FL: Krieger Publishing Company.

Fitch H.S., Fleet R.R. 1970. Natural history of the milk snake (*Lampropeltis triangulum*) in Northeastern Kansas. Herpetologica 26:387–396.

Fitzpatrick B.M., Fordyce J.A., Gavrilets S. 2009. Pattern, process and geographic modes of speciation. J. Evol. Biol. 22:2342–2347.

Fontanella F.M.M., Feldman C.R.R., Siddall M.E.E., Burbrink F.T. 2008. Phylogeography of *Diadophis punctatus*: Extensive lineage diversity and repeated patterns of historical demography in a trans-continental snake. Mol. Phylogenet. Evol. 46:1049–1070.

Frichot E., Mathieu F., Trouillon T., Bouchard G., François O. 2014. Fast and efficient estimation of individual ancestry coefficients. Genetics 196:973–983.

Frost D.R., Kluge A.G. 1994. A consideration of epistemology in systematic biology, with special reference to species. Cladistics 10:259–294.

Funk V.A., Akai A.K.S., Richardson A.K. 2002. Biodiversity: the interface between systematics and conservation. Syst. Biol. 51:235–237.

Gagnaire P.-A., Pavey S. a, Normandeau E., Bernatchez L. 2013. The genetic architecture of reproductive isolation during speciation-with-gene-flow in lake whitefish species pairs assessed by RAD sequencing. Evolution 67:2483–97.

Gehara M., Mazzochinni G.G., Burbrink F. 2020. PipeMaster: inferring population divergence and demographic history with approximate Bayesian computation and supervised machine-learning in R. bioRxiv.:2020.12.04.410670. Available from: https://doi.org/10.1101/2020.12.04.410670.

Ghiselin M.T. 1974. A radical solution to the species problem. Syst. Zool. 23:536–544.

Gower J.C. 1966. Some distance properties of latent root and vector methods used in multivariate analysis. Biometrika 53:325–338.

Guillot G., Rousset F. 2013. Dismantling the Mantel tests. Methods Ecol. Evol. 4:336–344.

Hall E.R., Kelson K.R. 1959. The mammals of North America. New York: Ronald Press.

Hanberry B.B. 2019. Defining the historical northeastern forested boundary of the Great Plains Grasslands in the United States. Prof. Geogr.

Harrington S.M., Hollingsworth B.D., Higham T.E., Reeder T.W. 2018. Pleistocene climatic fluctuations drive isolation and secondary contact in the red diamond rattlesnake (Crotalus ruber) in Baja California. J. Biogeogr. 45:64–75.

Harrison R.G. 1993. Hybrid zones and the evolutionary process. Oxford: Oxford University Press.

Harrison R.G., Larson E.L. 2014. Hybridization, introgression, and the nature of species boundaries. J. Hered. 105 Suppl 1:795–809.

He Z., Li X., Yang M., Wang X., Zhong C., Duke N.C., Wu C.-I., Shi S. 2019. Speciation with gene flow via cycles of isolation and migration: insights from multiple mangrove taxa. Natl. Sci. Rev. 6:275–288.

Hendry A.P., Nosil P., Rieseberg L.H. 2007. The speed of ecological speciation. Funct. Ecol. 21:455–464.

Hewitt G.M. 2000. The genetic legacy of the Quarternary ice ages. Nature 405:907–913.

Hewitt G.M. 2004. Genetic consequences of climatic oscillations in the Quaternary. Philos. Trans. R. Soc. Lond. B. Biol. Sci. 359:183–95; discussion 195.

Hewitt G.M. 2011. Quaternary phylogeography: the roots of hybrid zones. Genetica. 139:617–638.

Hey J. 2010. Isolation with migration models for more than two populations. Mol. Biol. Evol. 27:905–920.

Hijmans R.J., van Etten J., Checg J. 2014. raster: geographic data analysis and modeling [R package raster version 3.3-13]. Available from: https://rdrr.io/cran/raster/.

Hillis D.M. 2020. The detection and naming of geographic variation within species. Herpetol. Rev. 51:52–56.

Hudson R.R. 1983. Properties of a neutral allele model with intragenic recombination. Theor. Popul. Biol. 23:183–201.

Hudson R.R. 2002. Generating samples under a Wright-Fisher neutral model of genetic variation. Bioinformatics 18:337–338.

Hull D.L. 1976. Are species really individuals? Syst. Zool. 25:174–191.

Jackson N.D., Carstens B.C., Morales A.E., O'Meara B.C. 2017. Species delimitation with gene flow. Syst. Biol. 66:799–812.

Jaeger J.R., Riddle B.R., Bradford D.F. 2005. Cryptic Neogene vicariance and Quaternary dispersal of the red-spotted toad (Bufo punctatus): insights on the evolution of North American warm desert biotas. Mol. Ecol. 14:3033–3048.

Janèúchová-Lásková J., Landová E., Frynta D. 2015. Are genetically distinct lizard species able to hybridize? A review. Curr. Zool. 61:155–180.

Jombart T., Devillard S., Balloux F. 2010. Discriminant analysis of principal components: a new method for the analysis of genetically structured populations. BMC Genet. 11:94.

Karger D.N., Conrad O., Böhner J., Kawohl T., Kreft H., Soria-Auza R.W., Zimmermann N.E., Linder H.P., Kessler M. 2017.

Climatologies at high resolution for the earth's land surface areas. Sci. Data. 4:1–20.

Klicka J., Zink R.M. 1999. Pleistocene effects on North American songbird evolution. Proc. R. Soc. Lond. Ser. B 266:695–700.

Klopfstein S., Currat M., Excoffier L. 2006. The fate of mutations surfing on the wave of a range expansion. Mol. Biol. Evol. 23: 482–490.

Kozak K.H., Wiens J.J. 2006. Does niche conservatism promote speciation? A case study in North American salamanders. Evolution (NY) 60:2604–2621.

Kuhn M. 2008. Caret: classification and regression training package. R package version 6.0-77. 28. Available from: https://github.com/topepo/caret.

Kumar V., Lammers F., Bidon T., Pfenninger M., Kolter L., Nilsson M.A., Janke A. 2017. The evolutionary history of bears is characterized by gene flow across species. Sci. Rep. 7:46487.

Leaché A.D., Reeder T.W., Leache A.D., Reeder T.W. 2002. Molecular systematics of the Eastern Fence Lizard (Sceloporus undulatus): a comparison of parsimony, likelihood, and Bayesian approaches. Syst. Biol. 51:44–68.

Leaché A.D., Zhu T., Rannala B., Yang Z. 2019. The spectre of too many species. Syst. Biol. 68:168–181.

Legendre P., Fortin M.J. 2010. Comparison of the Mantel test and alternative approaches for detecting complex multivariate relationships in the spatial analysis of genetic data. Mol. Ecol. Resour. 10:831–844.

Legendre P., Oksanen J., ter Braak C.J.F. 2011. Testing the significance of canonical axes in redundancy analysis. Methods Ecol. Evol. 2:269–277.

Lek S., Delacoste M., Baran P., Dimopoulos I., Lauga J., Aulagnier S. 1996. Application of neural networks to modelling nonlinear relationships in ecology. Ecol. Model. 90:39–52.

Lek S., Guégan J.F. 1999. Artificial neural networks as a tool in ecological modelling, an introduction. 120:65–73.

Libbrecht M.W., Noble W.S. 2015. Machine learning applications in genetics and genomics. Nat. Rev. Genet. 16:321–332.

Ma Y., Wang J., Hu Q., Li J., Sun Y., Zhang L., Abbott R.J., Liu J., Mao K. 2019. Ancient introgression drives adaptation to cooler and drier mountain habitats in a cypress species complex. Commun. Biol. 2:213. doi: 10.1038/s42003-019-0445-z.

MacPherson A., Wang S., Yamaguchi R., Rieseberg L.H., Otto S.P. 2021. Parental population range expansion before secondary contact promotes heterosis. bioRxiv.:2020.04.28.066308. Available from: https://doi.org/10.1101/2020.04.28.066308.

Martin B.T., Douglas M.R., Chafin T.K., Placyk J.S., Birkhead R.D., Phillips C.A., Douglas M.E. 2019. Contrasting signatures of introgression in North American box turtle (Terrapene spp.) contact zones. Mol. Ecol. 29:4186–4202.

Mason A.J., Grazziotin F.G., Zaher H., Lemmon A.R., Moriarty Lemmon E., Parkinson C.L. 2019. Reticulate evolution in nuclear Middle America causes discordance in the phylogeny of palm-pitvipers (Viperidae: Bothriechis). J. Biogeogr. 46:833–844.

May R.M. 1990. Taxonomy as destiny. Nature 347:129–130.

Mayden R.L. 1988. Vicariance biogeography, parsimony, and evolution in North American freshwater fishes. Syst. Zool. 37:329.

Mayden R.L. 2002. On biological species, species concepts and individuation in the natural world. Fish Fish. 3:171–196.

Mayr E. 1963. Animal species and evolution. Cambridge: Belknap Press of Harvard University Press.

Mishler B.D., Donoghue M.J. 1982. Species concepts-a case for pluralism. Syst. Zool. 31:491–503.

Morrison W.R., Lohr J.L., Duchen P., Wilches R., Trujillo D., Mair M., Renner S.S. 2009. The impact of taxonomic change on conservation: does it kill, can it save, or is it just irrelevant? Biol. Conserv. 142:3201–3206.

Muller H.J. 1942. Isolating mechanisms, evolution and temperature. Biological Symposia Volume 6. Temperature and evolution. Isolating mechanisms. Genetic control of Embryonic development. Biological Symposia. A Series of Volumes Devoted to Current Symposia in the Field of Biology. Lancaster, Pennsylvania: Jacques Cattell Press. p. 71–125.

Myers E.A., McKelvy A.D., Burbrink F.T. 2020. Biogeographic barriers, Pleistocene refugia, and climatic gradients in the southeastern

Nearctic drive diversification in cornsnakes (*Pantherophis guttatus* complex). Mol. Ecol. 29:797–811.

Nguyen L.-T., Schmidt H.A., von Haeseler A., Minh B.Q. 2015. IQ-TREE: a fast and effective stochastic algorithm for estimating maximum-likelihood phylogenies. Mol. Biol. Evol. 32:268–274.

Nosil P. 2012. Ecological speciation. Oxford: Oxford University Press.

Nosil P., Feder J.L. 2012. Genomic divergence during speciation: causes and consequences. Philos. Trans. R. Soc. B Biol. Sci. 367:332–342.

Nosil P., Funk D.J., Ortiz-Barrientos D. 2009. Divergent selection and heterogeneous genomic divergence. Mol. Ecol. 18:375–402.

Orr H.A., Turelli M. 2001. The evolution of postzygotic isolation: accumulating Dobzhansky-Muller incompatibilities. Evolution 55:1085–1094.

Payseur B.A., Rieseberg L.H. 2016. A genomic perspective on hybridization and speciation. Mol. Ecol. 25:2337–2360.

Pereira P., Teixeira J., Velo-Antón G. 2018. Allele surfing shaped the genetic structure of the European pond turtle via colonization and population expansion across the Iberian Peninsula from Africa. J. Biogeogr. 45:2202–2215.

Phillips S.J., Dudik M. 2008. Modeling of species distributions with Maxent: new extensions and a comprehensive evaluation. Ecography (Cop.) 31:161–175.

Placyk J.S., Fitzpatrick B.M., Casper G.S., Small R.L., Reynolds R.G., Noble D.W.A., Brooks R.J., Burghardt G.M. 2012. Hybridization between two gartersnake species (*Thamnophis*) of conservation concern: a threat or an important natural interaction? Conserv. Genet. 13:649–663.

Plummer M., Best N., Cowles K., Vines K. 2006. CODA: convergence diagnosis and output analysis for MCMC. R News 6:7–11.

Powell R., Conant R., Collins J.T. 2016. Peterson field guide to reptiles and amphibians of eastern and central North America. Boston: Houghton Mifflin Harcourt.

Prance G.T. 1995. Systematics, conservation and sustainable development. Biodivers. Conserv. 4:490–500.

Pyron R.A., Burbrink F.T. 2009. Systematics of the Common Kingsnake (*Lampropeltis getula*; Serpentes: Colubridae) and the burden of heritage in taxonomy. Zootaxa 2241:22–32.

Pyron R.A., Burbrink F.T. 2010. Hard and soft allopatry: physically and ecologically mediated modes of geographic speciation. J. Biogeogr. 37:2005–2015.

Rangel T.F., Colwell R.K., Graves G.R., Fuèíková K., Rahbek C., Diniz-Filho J.A.F. 2015. Phylogenetic uncertainty revisited: implications for ecological analyses. Evolution (NY) 69:1301–1312.

Reding D.M.., Bronikowski A.M., E. J.W., Clark W.R. 2012. Pleistocene and ecological effects on continental-scale genetic differentiation in the bobcat (*Lynx rufus*). Mol. Ecol. 21:3078–3093.

Reding D.M., Castañeda-Rico S., Shirazi S., Hofman C.A., Cancellare I.A., Lance S.L., Beringer J., Clark W.R., Maldonado J.E. 2021. Mitochondrial genomes of the United States distribution of Gray Fox (Urocyon cinereoargenteus) reveal a major phylogeographic break at the Great Plains Suture Zone. Front. Ecol. Evol. 0:346.

Remington C.L. 1968. Suture-zones of hybrid interaction between recently joined biotas. Evolutionary biology. Boston, MA: Springer US. p. 321–428.

Reydon T.A.C. 2009. Species and kinds: a critique of Rieppel's "one of a kind" account of species. Cladistics 25:660–667.

Rising J.D. 1983. The Great Plains hybrid zones. Curr. Ornithol. Vol.1.:131–157.

Rissler L.J., Smith W.H. 2010. Mapping amphibian contact zones and phylogeographical break hotspots across the United States. Mol. Ecol. 19:5404–5416.

Roble S.M., Wooide G.N., Kinsler M.D. 2007. Discovery of a population of scarlet kingsnakes (*Lampropeltis triangulum elapsoides*) in the Virginia Piedmont. Catesbeiana 27:849–94.

Roux C., Fraïsse C., Romiguier J., Anciaux Y., Galtier N., Bierne N. 2016. Shedding light on the grey zone of speciation along a continuum of genomic divergence. PLoS Biol. 14:e2000234.

Ruane S. 2015. Using geometric morphometrics for integrative taxonomy: an examination of head shapes of milksnakes (genus *Lampropeltis*). Zool. J. Linn. Soc. 174:394–413.

Ruane S., Bryson R.W., Pyron R.A., Burbrink F.T. 2014. Coalescent species delimitation in milksnakes (genus *Lampropeltis*) and impacts on phylogenetic comparative analyses. Syst. Biol. 63:231–250.

Ruane S., Torres-Carvajal O., Burbrink F.T. 2015. Independent demographic responses to climate change among temperate and tropical milksnakes (Colubridae: Genus *Lampropeltis*). PLoS One 10:e0128543.

Rundle H.D., Nosil P. 2005. Ecological speciation. Ecol. Lett. 8:336–352.

Savage J.M. 1960. Evolution of a Peninsular Herpetofauna. Syst. Zool. 9:184.

Schilthuizen M. 2000. Dualism and conflicts in understanding speciation. Bioessays 22:1134–1141.

Schluter D. 2009. Evidence for ecological speciation and its alternative. Science (80-) 323:737–741.

Schoener T.W. 1968. The Anolis Lizards of Bimini: resource partitioning in a complex fauna. Ecology. 49:704–726.

Seeholzer G.F., Brumfield R.T. 2018. Isolation by distance, not incipient ecological speciation, explains genetic differentiation in an Andean songbird (Aves: Furnariidae: *Cranioleuca antisiensis*, Line-cheeked Spinetail) despite near threefold body size change across an environmental . Mol. Ecol. 27:279–296.

Servedio M.R., Hermisson J. 2020. The evolution of partial reproductive isolation as an adaptive optimum. Evolution (NY). 74:4–14.

Sheehan S., Song Y.S., Buzbas E., Petrov D., Boyko A., Auton A. 2016. Deep learning for population genetic inference. PLoS Comput. Biol. 12:e1004845.

Simpson G.G. 1951. The species concept. Evolution (NY) 5:285–298.

Slatkin M. 1993. Isolation by distance in equilibrium and non-equilibrium populations. Evolution (NY) 47:264–279.

Soltis D.E., Morris A.B., McLachlan J.S., Manos P.S., Soltis P.S. 2006. Comparative phylogeography of unglaciated eastern North America. Mol. Ecol. 15:4261–4293.

Stankowski S., Chase M.A., Fuiten A.M., Rodrigues M.F., Ralph P.L., Streisfeld M.A. 2019. Widespread selection and gene flow shape the genomic landscape during a radiation of monkeyflowers. PLoS Biol. 17:e3000391.

Streicher J.W., McEntee J.P., Drzich L.C., Card D.C., Schield D.R., Smart U., Parkinson C.L., Jezkova T., Smith E.N., Castoe T.A. 2016. Genetic surfing, not allopatric divergence, explains spatial sorting of mitochondrial haplotypes in venomous coralsnakes. Evolution (NY) 70:1435–1449.

Swenson N.G. 2006. Gis-based niche models reveal unifying climatic mechanisms that maintain the location of avian hybrid zones in a North American suture zone. J. Evol. Biol. 19:717–725.

Swenson N.G., Howard D.J. 2005. Clustering of contact zones, hybrid zones, and phylogeographic breaks in North America. Am. Nat. 166:581–591.

Van der Vaart A.W. 1998. Asymptotic statistics. Cambridge, UK: Cambridge University Press.

Vavrek M.J. 2020. Fossil. Available from: https://cran.r-project.org/web/packages/fossil/index.html.

Velasco J.D. 2008. Species concepts should not conflict with evolutionary history, but often do. Stud. Hist. Philos. Sci. Part C Stud. Hist. Philos. Biol. Biomed. Sci. 39:407–414.

Walker D., Avise J.C. 1998. Principles of phylogeography as illustrated by freshwater and terrestrial turtles in the southeastern United States. Annu. Rev. Ecol. Syst. 29:23–58.

Waltari E., Hijmans R.J., Peterson A.T., Nyári Á.S., Perkins S.L., Guralnick R.P. 2007. Locating Pleistocene refugia: comparing phylogeographic and ecological niche model predictions. PLoS One 2:e563.

Warren D.L., Glor R.E., Turelli M. 2008. Environmental niche equivalency versus conservatism: quantitative approaches to niche evolution. (vol 62, pg 2868, 2008). Evolution (NY) 62:2868–2883.

Warren D.L., Glor R.E., Turelli M. 2010. ENMTools: a toolbox for comparative studies of environmental niche models. Ecography (Cop.) 33:607–611.

Wieringa J.G., Boot M.R., Dantas-Queiroz M. V., Duckett D., Fonseca E.M., Glon H., Hamilton N., Kong S., Lanna F.M., Mattingly K.Z., Parsons D.J., Smith M.L., Stone B.W., Thompson C., Zuo L., Carstens B.C. 2020. Does habitat stability structure intraspecific genetic diversity? It's complicated... Front. Biogeogr. 12:e45377. doi: 10.21425/F5FBG45377.

Williams K.L. 1988. Systematics and natural history of the American Milksnake, *Lampropeltis triangulum*. Milwaukee, WI: Milwaukee Public Museum.

Wollenberg Valero K.C., Marshall J.C., Bastiaans E., Caccone A., Camargo A., Morando M., Niemiller M.L., Pabijan M., Russello M.A., Sinervo B., Werneck F.P., Sites J.W. Jr., Wiens J.J., Steinfartz S. 2019. Patterns, mechanisms and genetics of speciation in reptiles and amphibians. Genes (Basel) 10:646.

Wright S. 1943. Isolation by distance. Genetics 28:114–38.

Zellmer A.J., Hanes M.M., Hird S.M., Carstens B.C. 2012. Deep phylogeographic structure and environmental differentiation in the carnivorous plant *Sarracenia alata*. Syst. Biol. 61:763–777.

Zhang W. 2010. Computational ecology: artificial neural networks and their applications. Hackensack (NJ): World Scientific Publishing Company.